Ann. Geophys., 27, 1153–1173, 2009
www.ann-geophys.net/27/1153/2009/

Annales Geophysicae

Arctic tidal characteristics at Eureka (80° N, 86° W) and Svalbard (78° N, 16° E) for 2006/07: seasonal and longitudinal variations, migrating and non-migrating tides

A. H. Manson[1], C. E. Meek[1], T. Chshyolkova[1], X. Xu[1], T. Aso[2], J. R. Drummond[3], C. M. Hall[4], W. K. Hocking[5], Ch. Jacobi[6], M. Tsutsumi[2], and W. E. Ward[7]

[1]Institute of Space and Atmospheric Studies, University of Saskatchewan, Saskatoon, Canada
[2]National Institute for Polar Research, Tokyo, Japan
[3]Physics and Atmospheric Science Department, University of Dalhousie, Halifax, Canada
[4]Tromso Geophysical Observatory, University of Tromso, Tromso, Norway
[5]Physics and Astronomy Department, University of Western Ontario, London, Canada
[6]Institute for Meteorology, University of Leipzig, Germany
[7]Physics and Astronomy Department, University of New Brunswick, Fredericton, Canada

Received: 4 September 2008 – Revised: 22 January 2009 – Accepted: 10 February 2009 – Published: 9 March 2009

Abstract. Operation of a Meteor Radar at Eureka, Ellesmere Island (80° N, 86° W) began in February 2006. The first 12 months of wind data (82–97 km) are combined with winds from the Adventdalen, Svalbard Island (78° N, 16° E) Meteor Radar to provide the first contemporaneous longitudinally spaced observations of mean winds, tides and planetary waves at such high Arctic latitudes. Unique polar information on diurnal non-migrating tides (NMT) is provided, as well as complementary information to that existing for the Antarctic on the semidiurnal NMT.

Zonal and meridional monthly mean winds differed significantly between Canada and Norway, indicating the influence of stationary planetary waves (SPW) in the Arctic mesopause region. Both diurnal (D) and semi-diurnal (SD) winds also demonstrated significantly different magnitudes at Eureka and Svalbard. Typically the D tide was larger at Eureka and the SD tide was larger at Svalbard. Tidal amplitudes in the Arctic were also generally larger than expected from extrapolation of high mid-latitude data. For example time-sequences from ∼90 km showed D wind oscillations at Eureka of 30 m/s in February–March, and four day bursts of SD winds at Svalbard reached 40 m/s in June 2006.

Fitting of wave numbers for the migrating and non-migrating tides (MT, NMT) successfully determines dominant tides for each month and height. For the diurnal tide, NMT with s=0, +2 (westward) dominate in non-summer months, while for the semi-diurnal tide NMT with s=+1, +3 occur most often during equinoctial or early summer months. These wave numbers are consistent with stationary planetary wave (SPW)-tidal interactions.

Assessment of the global topographic forcing and atmospheric propagation of the SPW (S=1, 2) suggests these winter waves of the Northern Hemisphere are associated with the 78–80° N diurnal NMT, but that the SPW of the Southern Hemisphere winter have little influence on the summer Arctic tidal fields. In contrast the large SPW and NMT of the Arctic winter may be associated, consistent with Antarctic observations, with the observed occurrence of the semidiurnal NMT in the Antarctic summer.

Keywords. Atmospheric composition and structure (Middle atmosphere – composition and chemistry) – Meteorology and atmospheric dynamics (Polar meteorology; Waves and tides)

1 Introduction

Our global knowledge and understanding of solar atmosphere tides has been strongly influenced by the geographical distribution of continents and islands, but also by historical, national, economic and cultural realities. These factors that dominate ground-based observational systems have become less important as space-based technologies were

Correspondence to: A. H. Manson
(alan.manson@usask.ca)

developed during the 1990s. Such satellite data are most useful in providing information on migrating tides (MT), which are the zonal (longitudinal) mean tides, and also non-migrating-tides (NMT) from equator to medium-high latitudes (40–70°); e.g. Manson et al. (2004a), Forbes and Wu (2006), Zhang et al. (2006). The temporal resolution of satellite systems is also generally quite restricted, with seasonal means tending to dominate the results. In contrast ground-based observations, using "meteor winds" (VHF systems; MWR) and "medium frequency" radars (MFR), provide both good height sampling (circa 80–100 km, 2–3 km resolution) and high temporal resolution (1–2 day mean of winds and tides) for years and, for some locations, several solar cycles, e.g. Collm, 51° N; Saskatoon, 52° N, Adelaide 35° S, Christchurch 45° S. These location-specific solar tides are combinations of not only the various tidal Hough modes making up the MT, but also NMT, so that observed tidal amplitudes, phases and vertical wavelengths vary with longitude and season (Manson et al., 2006; Cierpik et al., 2003), due to the spatial and temporal variability of NMT-forcing by cumulonimbus clouds (e.g. Forbes et al., 2003; Oberheide and Forbes, 2008) and stationary planetary waves (SPW: Hagan and Roble, 2001).

Returning to geographical and historical factors, the birth of the personal computer (PC) has led to the above mentioned extensive radar archives reaching from circa 1978. Somewhat randomly placed radars now extend from equator to Arctic latitudes, including the two recently installed radars that are the focus of this paper. The irregularly shaped Arctic Ocean precludes longitudinal networks north of 65–70° N, although some studies exist using six or so of such temporally contemporaneous systems near those latitudes (Portnyagin et al., 2004). However, the absence of coverage in north-eastern Russia and the longitudinal extent of the northern Pacific Ocean (a 140° data gap) have made identification of NMT difficult. Portnyagin et al. (2004) concluded that the migrating tides (diurnal D and semi-diurnal SD) are dominant in the southern Arctic (65–70° N), but with some indications of NMT. These latter were based on the modest departures from slopes of 1 and 2, respectively (corresponding to the MT, s=+1 and +2) for the plots of D and SD phases (time of maximum in UT) versus longitudes. Positive wave-numbers are westward propagating, with the sun. Preferences for semidiurnal NMT were May and June, while for the diurnal NMT weaker preferences were November, January and February. This paper will show that these preferences are quite similar to the months for which NMT were determined, based upon our analysis of the Svalbard and Eureka Arctic tides near 80° N during 2006/07. Another paper by Wu et al. (2003) relied upon EISCAT-Tromso radar data (70° N) and optical interferometers at Resolute Bay (75° N) and Eureka (80° N), showing only two days of winter (January) data. Points of note are that 12-h oscillations were weak and not the dominant waves in Canada (we will later show supporting evidence for this at 80° N), and secondly that the Tromso-Resolute 12-h phases were consistent with SD s=+2 migrating tides. Also the SD tidal phases at Eureka, compared to Tromso, fitted neither s=+1 or +2 well.

In contrast, the Southern Hemisphere (SH), while suffering geographically at middle latitudes, has the Antarctic continent as its star, which provides ideal observational sites along the coast from 68–78° S and also centered at the pole ("South Pole" station). Enthusiasm to share the riches of the continent has provided up to five contemporaneous radars over the last 2 decades, more evenly spaced than in the NH, but still with a 120° longitudinal gap. Murphy et al. (2006) used these five radars plus early data from two others (plus assumptions of year to year stationarity) to identify a dominant semidiurnal NMT of s=+1 (and a lesser s=0) during summer-equinox months (October–March). The regional average latitude was 69° S. They were did not demonstrate the presence of NMT for the diurnal tide away from the pole, as their monthly mean profiles (amplitude and phase) for the "outer rim" (67–78° S) of MF radars were significant for the MT (s=+1) only. They also showed 12-monthly amplitudes at 94km for the outer rim and the South Pole; these were very similar and they concluded that this "verified predictions that the amplitude of the s=+1 component should remain constant with (high) latitude. . . ."

Earlier substantial polar tidal studies were all centered on "South Pole" and those results are relevant to our new studies at Eureka and Svalbard in the NH. Hernandez et al. (1993) used OH emissions for several winter-years and identified a 12-h oscillation of s=+1. A meteor radar at 90° S (Forbes et al., 1995) that used orthogonal antennas provided confirmation of a 12-h NMT with s=+1, and their preference for process was non-linear interactions with the local summer stationary planetary wave (SPW) with S=+1. This latter is consistent with an off-set polar vortex, and the inherent presence of the migrating SD s=2 at nearby high latitudes (i.e. circa 70° S or Antarctic latitudes). A more recent paper (Portnyagin et al., 1998) involved additional 90° S data for 1995/96 and 1996/97, plus radar data from Scott Base (78° S), Molodezhnaya and Mawson (68° and 67° S). At "South Pole" the 12-h oscillations were consistent with a NMT of s=+1 for spring-summer months: the oscillations had variable seasonal amplitudes ranging from 5–10 m/s (mid-summer) to 15–20 m/s; smooth phase-trends of several hours from spring to summer; and day-to-day variations (5–10 m/s) of tidal amplitudes with periods in the planetary wave range (circa 5 to 8 days). The 90° S winter oscillations were non-solar related and of period 6–11.5 h. Regarding the diurnal tide, a 24-h oscillation was observed in all months, but with weaker amplitudes in winter; Portnyagin et al. (1998) suggested that it was probably connected with the evanescent MT with s=+1. Away from the pole, the 12-h oscillation at Scott Base (78° S) was also consistent with a dominant NMT of s=1 and shared spring and summer maximum amplitudes seen at South Pole. In contrast at 68° and 67° S the SD tides had maximum equinoctial amplitudes and

a mixture of MT (s=+2) and NMT (s=+1) was suggested. They finished by asking whether the semi-diurnal NMT s=1 is also present in the Arctic. Our answer to this question will be shown to be affirmative.

Some valuable modelling has been carried out recently. Aso (2000) has stressed the dominant role of evanescent diurnal modes (1,−1, 1,−2) of the MT at polar mesopause heights, and also the likely role of diurnal NMT at polar latitudes. Yamashita et al. (2002) used the Kyushu University GCM to confirm that "non-linear interaction with SPW is taking place", providing the 12-h NMT with s=+1. Their related calculations with this tide indicated that, once excited in the NH winter hemisphere, it could propagate to the polar MLT region of the SH and provide the local summer enhancement of the NMT s=+1. Most recently, Aso (2007) assessed the semi-diurnal NMT at polar latitudes using a linearized steady and explicit tidal model and confirmed the trans-equatorial propagation of the 12-h NMT with s=+1, which is forced in the opposite winter hemisphere. After discussing the asymmetry of the SPW S=+1 activity between the NH and SH, the authors suggested that a hemispheric asymmetry might also then exist in the seasonal variations of the semidiurnal NMT s=+1. We were reminded by two referees of the important and pertinent work of Baumgaertner et al. (2006): they provided amplitudes of the 12-h NMT with s=+1, and also the MT with s=+2, based upon observations at Scott Base (78° S) with an MF radar and at Halley (76° S) with an imaging radar Doppler interferometer. Consistent with the material in the first part of this paragraph, they showed that amplitudes of the NMT and the global SPW S=+1 were positively correlated near 1 hPa during the NH-winter months of November–February; but also near 10 hPa during the SH-winter-centred months of 7 April to 7 September. Our paper will allow this matter to be further investigated.

A recent paper by Forbes and Wu (2006) contains figures and discussion on much of the global tidal field (70° S–70° N), using temperatures from UARS-MLS (1991–1997) at heights of 25–86 km. Their study confirms the presence of diurnal NMT s=0, +2, −3 and semidiurnal NMT s=+1 and +3; the s=0 and +2 diurnal tides were not resolvable earlier from HRDI winds data, although the spectra were wide and their presence was suspected (Manson et al., 2004a). Although these NMT are tides in the temperature-field, their presence confirms their production processes as being SPW and/or latent heat release with wave numbers S=1 and 2. Their paper discusses at some length the development of a latitude-month temperature-contour comparison at 86 km between the 24-h NMT s=−3 from MLS-temperatures, and contours derived from their Hough Mode Extension fit to winds at 95 km using data WINDII (Wind Imaging Interferometer) and HRDI (High-Resolution Doppler Imager). While successfully indicating the combined utilization of space based winds and temperature for characterization, the authors do not discuss the differences between the latitudinal structures of this NMT in the temperature and winds fields. For example, Fig. 10 from Forbes and Wu (2006) shows little or no presence of the diurnal s=0 and +2 thermal-tides at 60–70° N throughout the year, in contrast with the relatively large amplitudes in the Southern Hemisphere; and their Fig. 11 suggests minimal presence of semidiurnal s=+1 thermal tide at high northern latitudes. However, the latitudinal structures of relevant "expansion functions" for winds and temperature do differ. Also the latitudinal variations of the diurnal Hough functions for various wave numbers (MT and NMT) are significant and the amplitudes for trapped modes are relatively more important at high latitudes (their Fig. 6). Hence, consistency between Figs. 10 and 11 of Forbes and Wu (2006) and the NMT characteristics for the winds that we will show for 78–80° N will not necessarily occur. It remains interesting, that as indicated in our summarizing and detailed Abstract, all three NMT wave numbers were dominant in the Arctic mesospheric winds near 80° N during 2006/07.

It is useful here to summarize 12-h/SD and 24-h/D tidal characteristics for extra-tropical and high (50–70° N) latitudes. Manson et al. (2002) used multi-year MF radar observations from 2–70° N and modeled tides (Global Scale Wave Model, GSWM; Canadian GCM, CMAM). The diurnal tide dominates from 2–35°, with maxima near 20°, equinoctial maxima, modest monthly phase changes, and wavelengths that are short (<30 km), long or evanescent (100+ km) at low and high latitudes, respectively. At 70° N (Tromso) the diurnal tidal amplitudes are very small (∼10 m/s below 90 km), as might be expected, since evanescent Hough modes of the migrating tide have begun to dominate over the propagating modes. The diurnal tides (combinations of all modes) are also small at these latitudes in the GSWM and CMAM (Manson et al., 2002). The semi-diurnal tide dominates above 35° (maxima near 50°), with winter and late summer-fall (August–October) seasonal maxima, large phase changes between solstices, and wavelengths that are 30–60 km in winter but long or irregular (≥100 km) in summer months. Again the combination of Hough modes provides decreasing amplitudes at higher latitudes; thus Tromso values (Manson et al., 2002, 2004b) range from 10 to 20 m/s (monthly means). Hence, in the absence of non-migrating tides, the D and SD amplitudes at Eureka and Svalbard were expected, at the time when the first 2 authors began supervision/operation of the Eureka radar in 2006, to be smaller than those at Tromso. We include the tides from the Svalbard radar in this statement, as results from there had not been published in 2006/07.

In this paper all aspects of tidal variability at Eureka and Svalbard are studied and compared. This is already the largest data archive of 78–80° polar contemporaneous winds in existence globally, featuring well-spaced (∼100°) longitudes through Norway and Canada. The radars are briefly described in Sect. 2. Our goal in Sect. 3 is to investigate the tidal spectra and time-sequences of the winds at Eureka (80° N, the newest radar) and Svalbard (78° N, from where no tidal results have yet been displayed). These are

compared with tides at two typical high mid-latitude locations, whose longitudes are similar to those of the two Arctic radars: Saskatoon (52° N) and Collm (51° N). The focus of Sect. 4 is a completely unique one: comparison of the first height (82–97 km) versus time (12 months of 2006/07) contour plots of diurnal (D) and semidiurnal (SD) tidal amplitudes and phases at two arctic (effectively equal) latitudes and differencing longitudes (16° E and 86° W). The initial indications of the non-migrating tides (NMT) are considered at this stage. The goal of Sect. 5 is to develop the longitudinal differences in tidal characteristics at Eureka and Svalbard into quantitative estimates of the seasonal and altitudinal variations of the NMT and their relative importance compared with the migrating tides (MT). Specific values of the zonal wave- numbers for NMT of the D and SD tides are provided. Zonal wave numbers of the topography and lower stratospheric winds are also provided in Sect. 6 and are linked to the SPW S=+1. This wave provides probable forcing and coupling of the NMT in the Northern and Southern Hemispheres (NH, SH). Section 7 provides a brief introduction to the importance of transient planetary waves in the upper middle atmosphere. A summary of the significant progress made in achieving the goals of this paper is provided in Sect. 8.

2 Radar systems and data analysis

We use two MWR radars of similar design (Hall et al., 2003; Hocking, 2005). Commercially the radar at Eureka (80° N, 86° W) is known as a SKiYMET system, which was developed and deployed by MARDOC-Incorporated (Modular Antenna Radar Designs of Canada). It is located at the Canadian Network for the Detection of Atmospheric Change (CANDAC) Polar Environmental and Atmospheric Research Laboratory (PEARL) on Ellesmere Island, Canada. The Svalbard (78° N, 16° E) radar was built by the National Institute of Polar Research (NIPR) in Japan in 2001, and is called NSMR (Nippon Scandinavia Meteor Radar). Relevant analyses of 2006/07 data were prepared by the first two authors for this joint circumpolar analysis.

In these cases of very high geographic latitudes, in particular during the winter months, the MWR initially appears to have an advantage over the otherwise competitive MFR. The latter are dominant in Antarctica. During these months the D-region ionization for the MFR-scatter is mainly provided by particle influx associated with auroral or polar cap disturbances, which are functions of solar activity and geomagnetic latitude (Nozawa et al., 2002). Some discussion on this possibility is appropriate. Indeed, tides over 12-month calendar years have been obtained at Tromso (70° N), which is within the auroral zone (Manson et al., 2004b). We also note that Baumgaeterner et al. (2005) provide both 12-h and 24-h multi-year monthly tidal sequences and "all-year-averages" from Scott Base (78° S), and simply comment that the diurnal tide is generally "much smaller" than the semi-diurnal tide. Again, as noted earlier, Murphy et al. (2006) also discussed the diurnal tide obtained from fitting spatial tidal harmonics to data from 5 "outer rim" radars. Hence, there is no technical or physical reason why the radars operating in Antarctica would not have detected tidal signals consistent with diurnal NMT if they existed.

3 Spectra and time-sequences

It is useful to inspect spectra of the low frequency wind variations (6 h to 16 days), so as to discern whether tidal frequencies are visible and well defined. We have chosen two high mid-latitude radars (MFR at Saskatoon 52° N, 105° W and MWR at Collm 51° N, 15° E) as a contrast for the two polar radars. Tidal data from Svalbard have not yet been discussed in the literature, so the first two authors of this paper had no expectations for them while the figures in this paper were prepared.

In Fig. 1, the first month of data from Eureka (14 February–14 March 2006) has been used for zonal (EW) wind spectra at 85 and 88 km; matching data from the other 3 radars are added. The spectra result from a Fourier transform method for selected frequencies, which are chosen to be linear with the cube root of the frequency. The conversion equation is given in the figure caption. These spectral estimates are therefore spaced more closely at lower frequencies than the usual components, for better apparent resolution and easier perusal of the range of periods shown (Manson et al., 2002). The well known speed-bias in the MF radars is small at these Saskatoon-heights (Hall et al., 2005), so the Collm-Saskatoon differences, if any, are small. (The meridional (NS) wind spectra at each site are similar.) As is typical of mid-latitudes, the SD tide dominates the spectra in these winter-like months, and the 24-h and 8-h are comparable to each other. To our great surprise, the Arctic tides of Fig. 1 are not simply smaller spectral versions of mid-latitudes (as we had seen for years at Tromso), but provide large diurnal tides and small or negligible semidiurnal tides at Eureka, with quite the reverse at Svalbard! We have inspected preliminary data at those two polar sites for 2007 and the tides are similar to Fig. 1. The planetary wave activity (3–16 days) is quite large (3–6 m/s) at all locations.

We have also inspected spectral tides from two radars 5–8 degrees south of the polar radars. Tromso (70° N) generally has a larger winter SD tidal feature than the D, and the 12-h and 24-h amplitude peaks for this particular interval of 2006 are relatively very similar to Svalbard. In contrast at Resolute Bay (MWR, 75° N, 95° W), south of Eureka, the spectrum in February–March (not shown) has no significant 12-h feature, and the 24-h feature is close to noise (as at 52° N). We will not discuss data-analyses from these two other radars further in any detail, but focus upon Svalbard and Eureka due to their close and higher latitude similarity and radar-type. Also, the data from Resolute Bay is less continuous than that

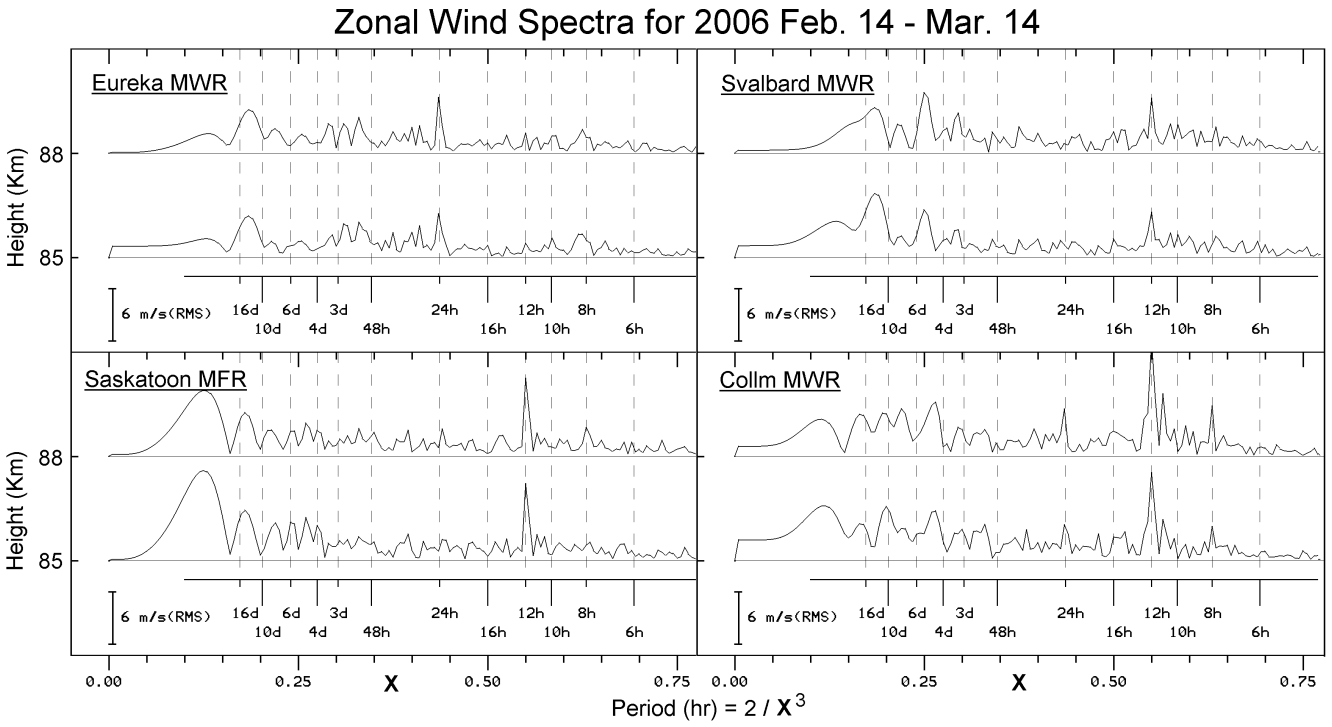

Fig. 1. Frequency spectra for two Arctic and two high mid-latitude radar-locations during winter months. The ordinate axis parameter is X, where the Period (h)=$2/X^3$=1/f, where f is the frequency in cycles per hour. This choice is discussed in the text, and provides better apparent resolution and easier perusal in the range of periods that are of interest.

from Eureka (they are to be discussed elsewhere); and the Tromso (MFR) tidal data, due to weaker radar scatter and auroral disturbances, can be somewhat noisy above 90 km. The latter has been discussed earlier in detail (Manson et al., 2004b), and the characteristics of the SD tides there are similar to those at middle latitudes, albeit of smaller amplitude and consistent with MT and tapering Hough-mode amplitudes. For example the Tromso diurnal tide is evanescent and has a weak summer maximum. Based upon Antarctic data as discussed in the Introduction, it was expected as this study was begun, that locations near 70° N could have a mixture of MT and NMT, whereas at Arctic latitudes (80–90° N) the NMT could be larger and even dominate.

We next provide two weeks of time sequences of the zonal wind (Fig. 2) for late spring/early summer months, chosen to represent winds from the other solstice but also because D and SD oscillations can be seen at both Arctic locations, as well as bursts of SD oscillations at Svalbard. There was also a strong ∼48-h oscillation (quasi 2 day wave; Q2DW) at Saskatoon and Collm at this time. From Fig. 2, at Eureka the SD tide is now visibly stronger than the D tide, although the D tide is evident also (day 159, near 94 km). In contrast, there are bursts of SD tide reaching 40 m/s amplitude at Svalbard (days near 153 and 160, 85–91 km). Inspection of the spectra for these sequences (Fig. 3) and of the spectra for Saskatoon and Collm, again show strong differences between mid-latitude and polar tidal oscillations. At 51/52° N the 12-h peaks are quite prominent, as expected, since there is usually a minor seasonal maximum in spring at these heights (Manson et al., 2006, 2004c), but there is no coherent (monthly mean) 24-h peak. Both sites feature Q2DW peaks. In fascinating distinction to winter, the Arctic spectra are now very similar to each other, with 12-h tides comparable to and even larger than at 51/52° N, and clear 24-h peaks (∼6 m/s) that are stronger than at mid-latitudes. On this occasion, again, the Tromso spectral features (not shown) were similar to Eureka, although somewhat weaker and noisier (less coherent over the month).

It is clearly time to assess the entire year, and it will be seen that the two intervals chosen (the first observing winter-month for Eureka, and an early summer month) are by no means typical.

4 Contour-climatologies and hodographs

Here we have used thirty-day fits for the 12 and 24-h tidal oscillations and means at Eureka and Svalbard. The fits have the first day of the month at their mid-point, and contours result from a bilinear interpolation procedure (Manson et al., 2006). The zonal and meridional amplitudes and (tidal) phases are provided in Figs. 4 and 5, respectively. Northward and eastward tidal winds are taken as positive, and the

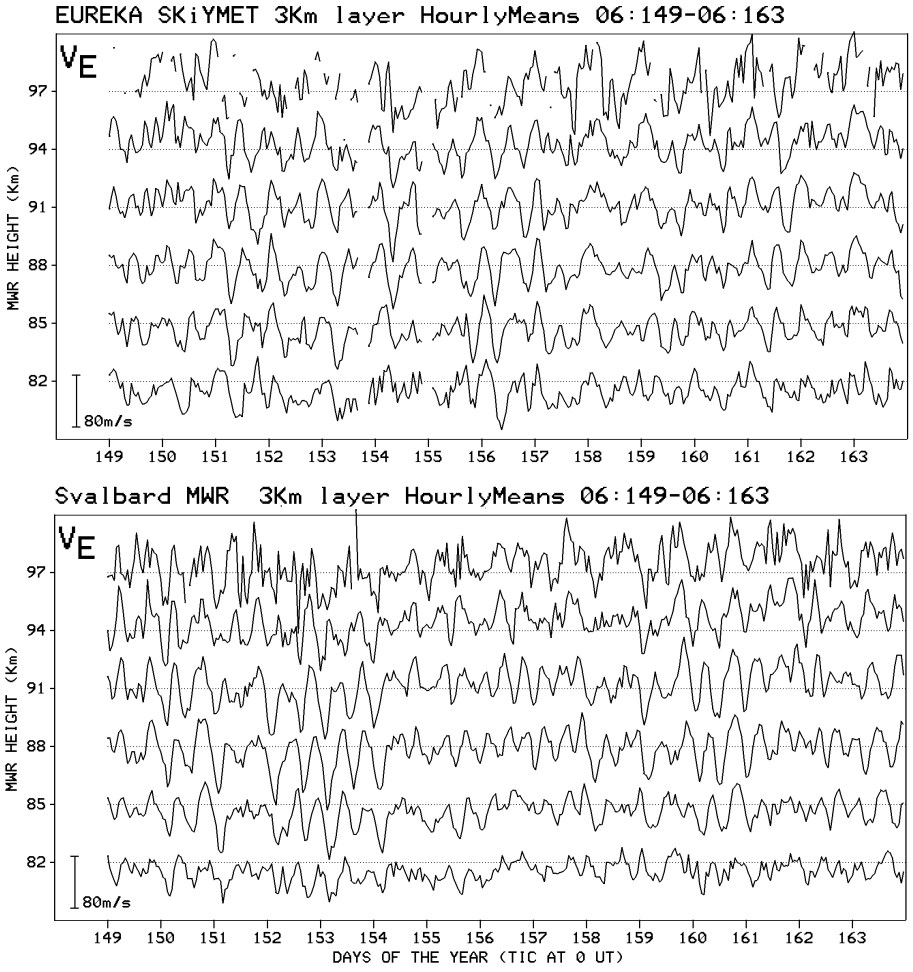

Fig. 2. Time sequences of the Zonal, or East-West winds.

phases are the local solar times of maximum northward and westward winds.

Regarding mean winds, the winter zonal vortex (Fig. 4) observed at Eureka is much stronger (by 10–15 m/s) than at Svalbard, while the Svalbard summer easterly (lower heights) and westerly (upper heights) circulations are stronger (by ∼5 m/s) than at Eureka. Generally the solstitial circulations at 51/52° N (Saskatoon and Collm are similar, and Saskatoon is shown) are much stronger, consistent with weaker meridional (NS) temperatures gradients and hence thermal winds at 80° N. The meridional winds in Fig. 5 are entirely consistent with the zonal winds and their vertical shears. The northward/southward flows of winter/summer lead to vertical motions at high latitudes, and hence to the warm/cool polar mesopause temperatures of winter/summer, which provide the observed westward/eastward vertical shears. Notice that summer southward Arctic flows are much stronger (by ∼4 m/s) than at high mid-latitudes, the former associated with strong divergence from the pole. In all three cases the peak NS flows are at the heights of maximum EW vertical eastward shear. The poleward winter flows are very strong in the Canadian sector, with Eureka illustrating even stronger convergence. Associated with the weak 2007 winter EW winds at Svalbard, the NS flows are either weak or reversed into equatorward flow. Similar effects were noted by Hall et al. (2003) in comparing the mean winds at Tromso and Svalbard, the coriolis torques on the meridional winds, and the linked GW-momentum drags. The upper heights of the polar vortex for 2006/07 were clearly not symmetrical about the North Pole. This will be addressed in vortex characterization studies (e.g. Chshyolkova et al., 2007) underway for the years 2006/07 and 2007/08.

Now considering the diurnal/24-h tide, and including in the discussions the hodographs of the tidal winds for 82 and 94 km (Figs. 6 and 7), we perceive extraordinary differences between middle and Arctic latitudes, and between Eureka and Svalbard in particular. The zonal wind spectra of Figs. 1 and 3 can now be placed in broader context: the contour-values for 1 March confirm the minimal (2–4 m/s) Svalbard

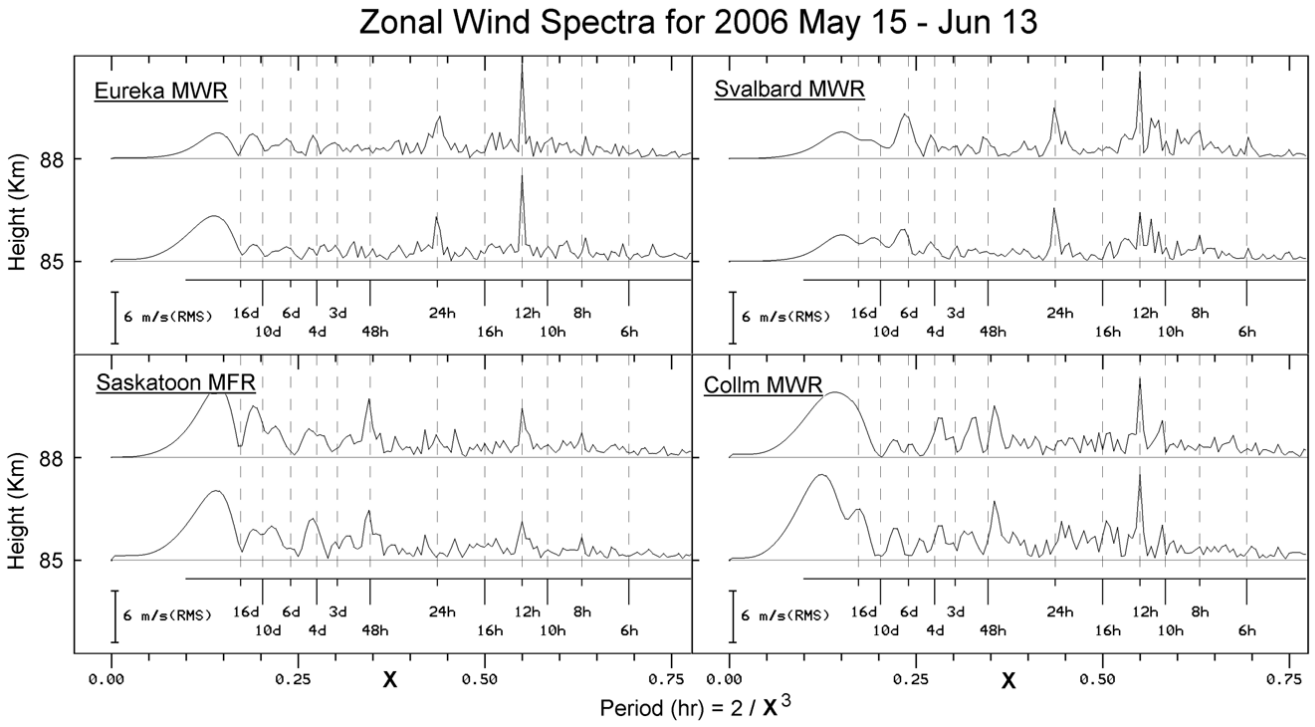

Fig. 3. Frequency spectra for two Arctic and two high mid-latitude radar-locations during early summer months. Otherwise the figure is configured identically to Fig. 1.

tide for both components and the large Eureka values; and for 1 June, at the lower heights, similar and modest amplitudes (8–10 m/s) at both sites. A deeper summer minimum occurred on 1 July. Quick inspection of 2007/08 revealed similar behaviour (not shown).

More significantly, some of the differences between the monthly values of diurnal tidal amplitudes and phases for the two Arctic locations are the largest we have ever seen. There are factors of nearly ten between the March amplitudes, with the zonal component providing the larger differences. The tidal variations with longitude near 40° N for the CUJO network (Manson et al., 2004c, 2006) were much smaller; and the hemispheric zonal patterns of amplitude and phase seen in HRDI satellite data from 96 km (Manson et al., 2004a), also for these lower latitudes, were significant but smaller. From the phase contours of Figs. 4 and 5 observed Arctic 24-h wavelengths (these involve superposition of the MT and NMT) are generally large compared with the shorter winter values at Saskatoon (52N) and often observed at other high mid-latitudes (Manson et al., 2002). However, Svalbard does have finite vertical gradients (∼120 km wavelength), while Eureka has only a consistent trend with time at all heights (8 h over 12 months). Differences in phase values (colors) between the Arctic radars are indicative of NMT effects, especially in the early spring of 2006, and the winter-centred months of 2006/07.

The hodographs of Figs. 6 and 7 provide a useful alternative perspective of the 24-h tide, with the two Arctic locations having quite similar elliptical-patterns and background wind vectors at 82 km, especially for the D tide, but having vastly different ellipses at 94 km, near where NMT are expected to begin their increased contribution to the locally observed tide (Forbes et al., 2003). The meridional axes amplitudes are quite similar (as in Fig. 5), but the very small zonal amplitudes have led to ellipses of large elongation. At 94 km the tidal hodographs differ dramatically from mid-latitudes, in this instance from the Saskatoon MFR. Superposition of MT and NMT of differing relative amplitude at different longitudes, and distortion of the classical tidal Hough modes by varying background winds, will lead to phase changes in the zonal and meridional components of the observed tides. The elliptical patterns will then depart from circularity. We have noted this in 96 km-tides from satellite data (Manson et al., 2004a), earlier radar data and tidal models for northern Scandinavia (Manson et al., 2004b), and in MFR data from Saskatoon (Manson et al., 2002).

Moving to the 12-h oscillation or SD tide in Figs. 4 and 5, the polar sites have more in common with the high mid-latitude's amplitudes and phase morphology: winter maxima along with the early fall (∼September) feature (Riggin et al., 2003), and somewhat similar large equinoctial changes of phases (colors) and associated vertical gradients. That said, Eureka's amplitudes are consistently smaller than at

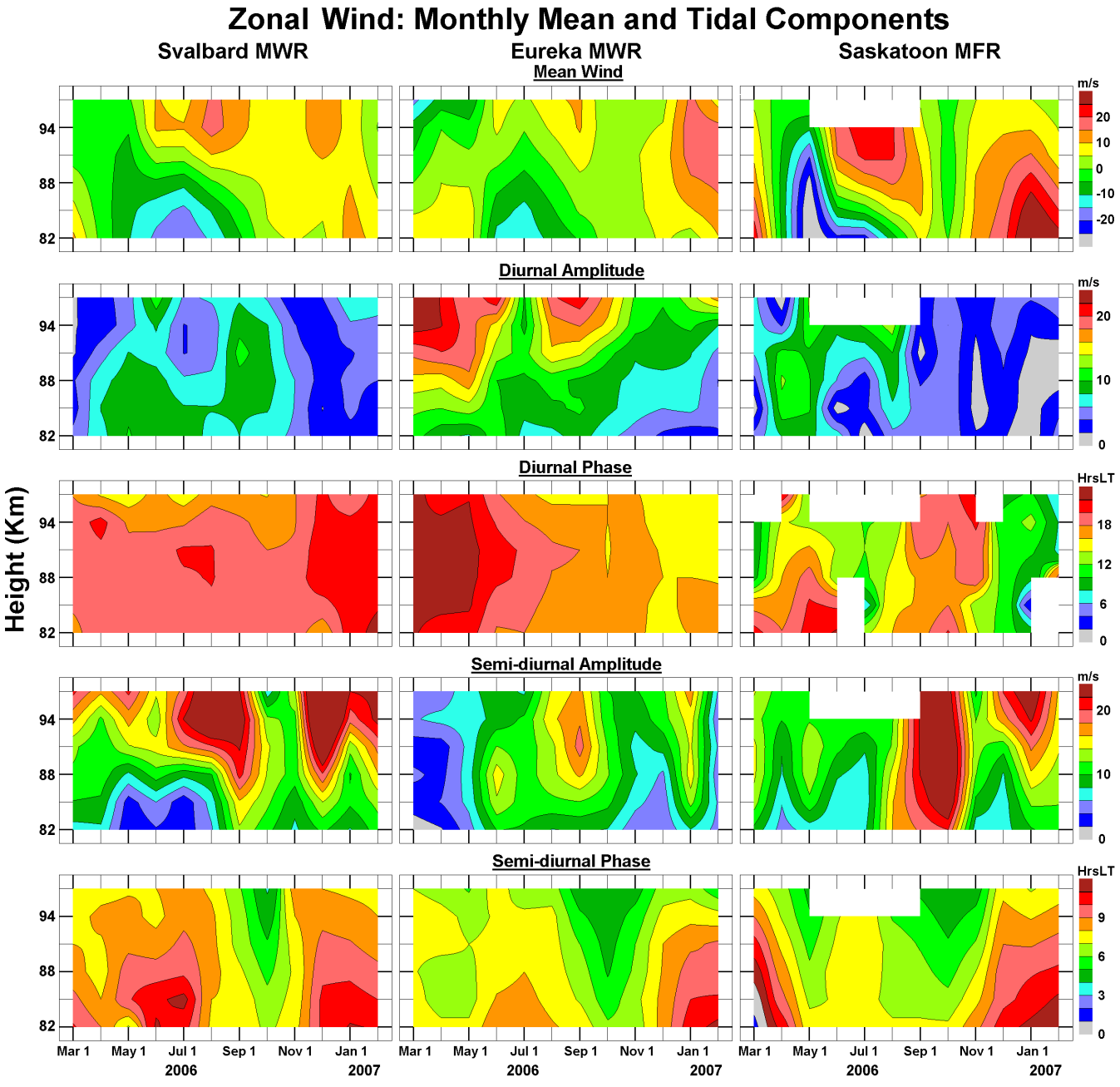

Fig. 4. Zonal winds for mean background winds and the tides, both diurnal (24-h) and semidiurnal (12-h). Eastward tidal winds are taken as positive, and the phases are the local solar times of maximum eastward winds. Heights above 94 km in mid-summer at Saskatoon are judged to be above the heights of total reflection for the MFR and therefore are not plotted.

Svalbard (half in September) and the deep Eureka-minimum in March led to the absence of a convincing spectral peak in Fig. 1. While NMT are manifested in this longitudinal phase-comparison, their impacts are likely to be smaller than for the diurnal tide, as inferred by Aso (2007).

Again the hodographs in Figs. 6 and 7 encapsulate a nice visual summary for the 12-h tide. At 82 km the 51/52° N SD tide is generally larger than the polar tides, with Eureka and Svalbard differing in the spring and some autumn months, thereby suggesting the presence of NMT. In contrast, at 94 km the polar tides are comparable in size to 52° N, with Svalbard having a dominant tide in late-summer/fall. This feature maximizes at different monthly times at the three sites. There are also generally large winter-centred values at the 3 sites. The tidal ellipses are more circular than for the D tide, which is consistent with orthogonal oscillations of the wind components.

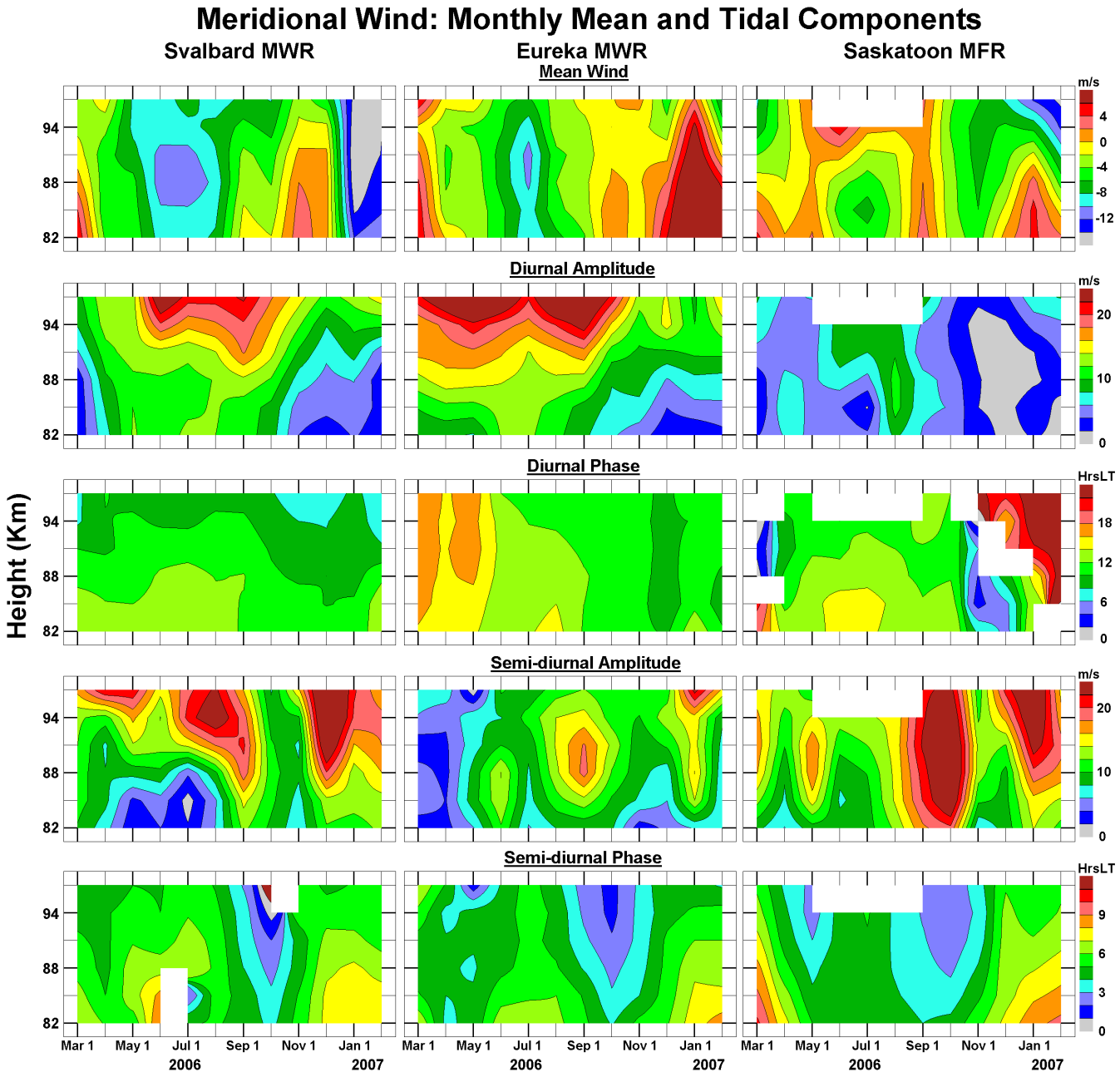

Fig. 5. Meridional winds for mean background winds and the tides, both diurnal (24-h) and semidiurnal (12-h). Northward tidal winds are taken as positive, and the phases are the local solar times of maximum northward winds. Heights above 94 km in mid-summer at Saskatoon are judged to be above the heights of total reflection for the MFR and therefore are not plotted.

5 Migrating (MT) and non-migrating tides (NMT)

This topic has been the focus of considerable research, discussions and papers in the last 10 years. While the role of NMT was a matter of conjecture by the radar community for some time, the references in the Introduction indicate recent studies confirming the significant presence of NMT, especially above 90 km, from both ground-based and space-based systems. Figure 8 provides the contours of monthly amplitude ratios S/E of Svalbard to Eureka, for diurnal and semi-diurnal tides, and differences (S-E) of mean winds and tidal phases: ratios of unity and phase-differences of zero are shown with a thicker contour-line.

The tidal amplitude ratios reinforce the figures and discussion of Sect. 4 very effectively. Generally, with few spatial disagreements, the Svalbard diurnal tide is much weaker month by month than at Eureka, especially for the EW

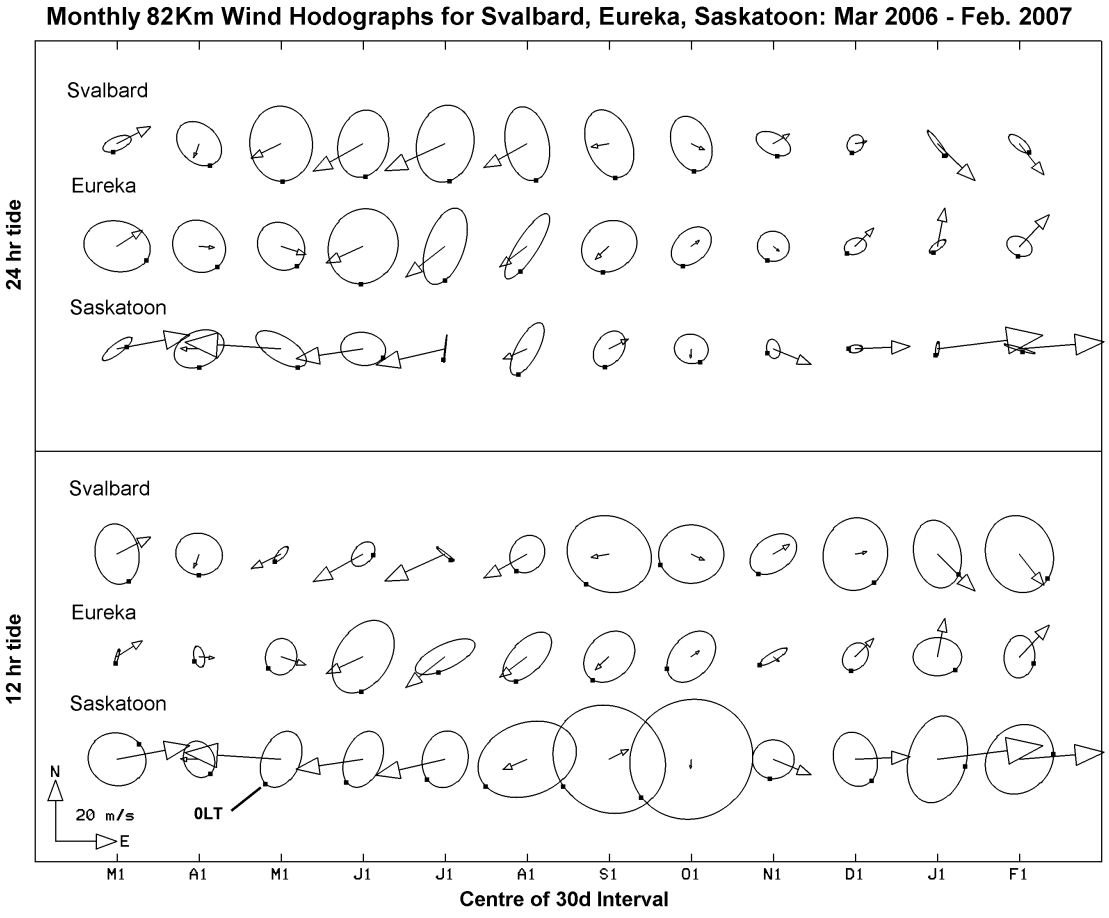

Fig. 6. Hodographs for the 24 and 12 h tidal components at 82 km from the Eureka and Svalbard radars along with those for the high mid-latitude MFR at Saskatoon (52 N). The arrows show the monthly mean winds, and the small black squares on the hodographs indicates the position of the tidal wind vector at 00:00 LT.

component. Again, except for the low altitude late spring-summer feature, the Svalbard semi-diurnal tide is much stronger than at Eureka. Regarding mean or background winds, the weakness of the Svalbard winter-westerlies and strength of the summer-easterlies, along with the unexpected winter-northerlies (2006/07) are strikingly evident.

Of fresh interest are the phases differences (hours) for the D tide, where the two greens on either side of the zero phase-difference line (thicker and darker) are on average within only ± 2 h of local time agreement (Fig. 8). The NS diurnal tide differences are thus probably consistent with migrating tide dominance (unless only amplitude modulation has occurred) for the large majority of months and heights after the 2006 spring; while the EW tide shows obvious NMT influence (phase modulation of more than ± 2 h) in the spring (2006) and winter (2007), with dark green and orange-pink colours. The amplitude ratios (S/E) are also large in the areas of consistently large phase differences (S-E). Manson et al. (2004a) showed, using the HRDI 96 km global tides, that both amplitudes and phases were significantly spatially/longitudinally modulated in the range of latitudes 40–70° (10–20 m/s, 06:00–08:00 LT), so similar or larger differences can be expected at these polar latitudes. Although we inspected time sequences of phase differences, which had higher temporal resolution due to the use of 4 days means, the variability was not so rapid or large as to favour its use. Our choice has been to include the useful and dominant NMT information based upon monthly means shown in Fig. 8. Finally, even though a large amplitude ratio means that one site has relatively small amplitudes (e.g. 2–4 m/s), the smooth appearances of monthly phases in Fig. 5 and especially differences in Fig. 8 suggest that both phases are reliable. No smoothing has been applied to these monthly data. Also, we have found (e.g. Manson et al., 2002) that differences between original time sequences of winds and the fits to the two tides plus the mean wind are consistent with gravity wave activity, rather than errors in the tidal fitting.

The semi-diurnal tide, which has quite circular hodographs all year for both polar locations, but generally much larger amplitudes at Svalbard, has significant

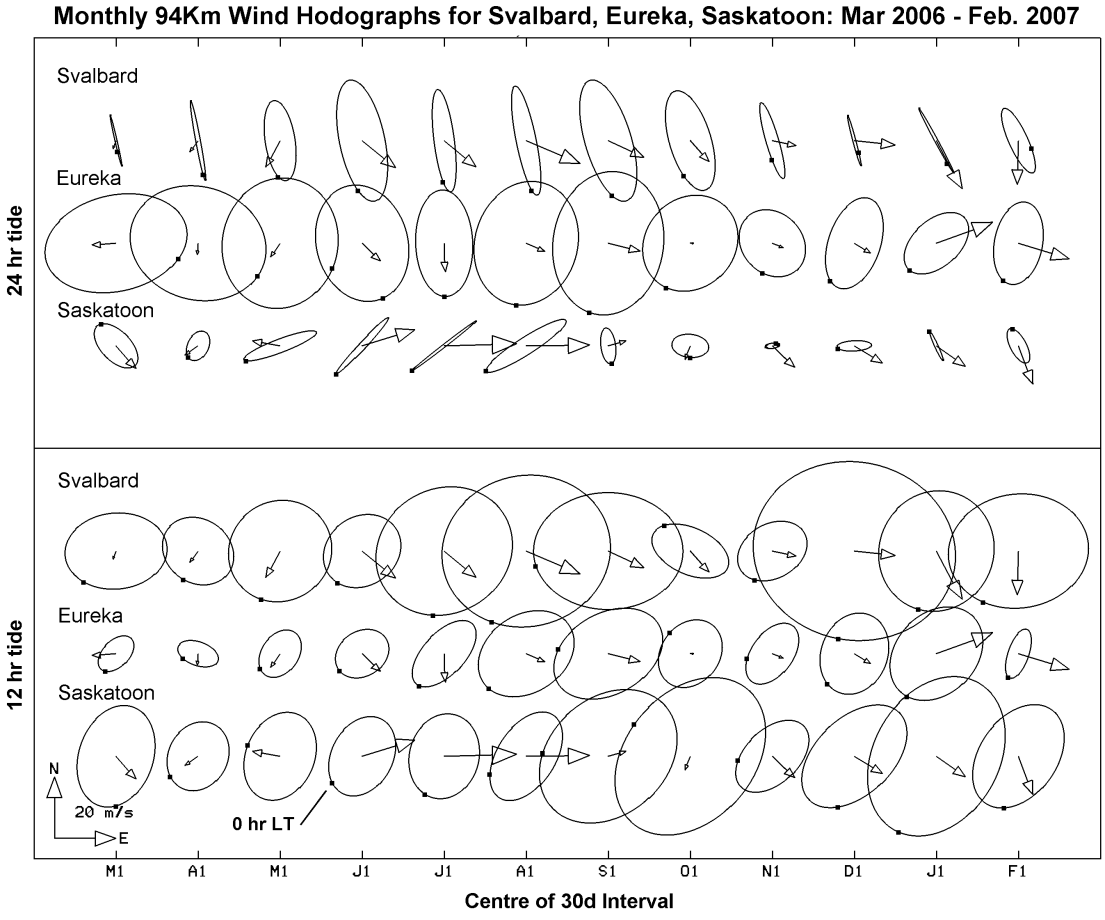

Fig. 7. Hodographs for the 24 and 12 h tidal components at 94 km from the Eureka and Svalbard radars along with those for the high mid-latitude MFR at Saskatoon (52 N). The arrows show the monthly mean winds, and the small black squares on the hodographs indicates the position of the tidal wind vector at 00:00 LT.

equinoctial areas of yellow/orange phase-differences (Fig. 8) in height and time, which are 1–4 h different from LT agreement. The amplitude ratios (S/E) are also large in these areas. NMT are thus expected in these height-time locations.

A migrating and non-migrating tide has been fitted to the data from the two sites. The amplitude and phase of the observed tide, which is made up of the MT and possibly several NMT, are known for the sites, as is the wave number of the MT i.e. s=+1 for the 24-h/D and s=+2 for the 12-h/SD. Since four observationally derived parameters are known it is possible to solve for the amplitude and phase of two tides (MT plus one NMT with a given wave number). With two sites the resulting set of equations has an exact solution, i.e. zero squared error, but it would be easy to add data from other sites (preferably at widely separated longitudes) so that the best non-migrating tide, i.e. minimum squared error, can be chosen. Unfortunately, it will not be easy to add another 80° N site. The program uses 12-months of data, with both monthly and 4 day fits available, for diurnal and semidiurnal tides and their EW and NS components at heights 82–97 km. A separate analysis from the program has also been used elsewhere to fit just the migrating tide (Manson et al., 2006); there we made statements such as "the migrating tide explains 60% of that period's tidal power". As stated, the fit of migrating and non-migrating tide is exact, that is, there is no reason that is based upon fit-error for selecting one pair over another. There is however justification for assuming one of the pair is a migrating tide, and hence MT/NMT values were calculated. Regarding the NMT, there are infinite possible choices for wave number, all of which will produce a solution. We regard very high wave numbers as unlikely to be coherent around the globe, especially over long periods such as a month, and so are left with the need to choose a limited wave number range. We have made this limitation based on expected stationary wave-tide interaction by-products. Given the previous discussion, when we fit an MT and NMT and find that one is stronger than the other we can argue that the stronger one in a single wave number fit would probably explain more than half the tidal "power". Considering that the choice of the dominant wave number in this

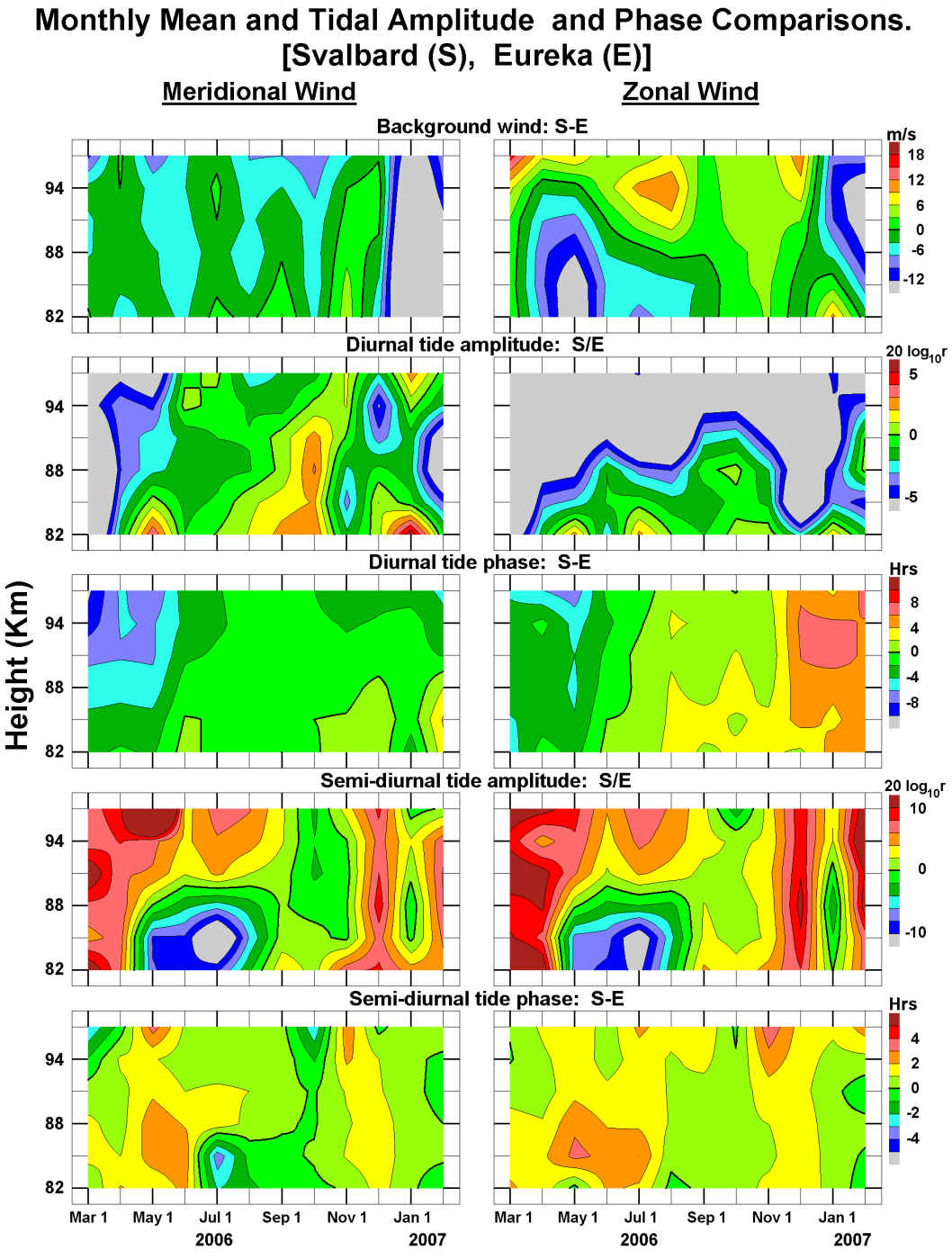

Fig. 8. Comparisons of the two Arctic radar monthly mean winds (differences in m/s), tidal amplitudes (expressed as the logarithmic ratio), and phase differences (of the local solar times).

way leads to regions in both height and month with the same wave number, we consider the method of choosing is justified given the limitation of 2 sites.

We have used the MT/NMT amplitude ratios in a selected NMT wave number range to determine the dominant tide: the MT is chosen if all ratios are greater than 1, or s is chosen for the NMT with the smallest MT/NMT ratio. While phases of the NMT were also available, we found that amplitude ratios allow easier discrimination between the dominant and weaker NMT. Thus Fig. 9 shows amplitude-ratio results from 12 monthly fits versus 6 heights (72 height-month locations) for each tidal component; if the MT is dominant the

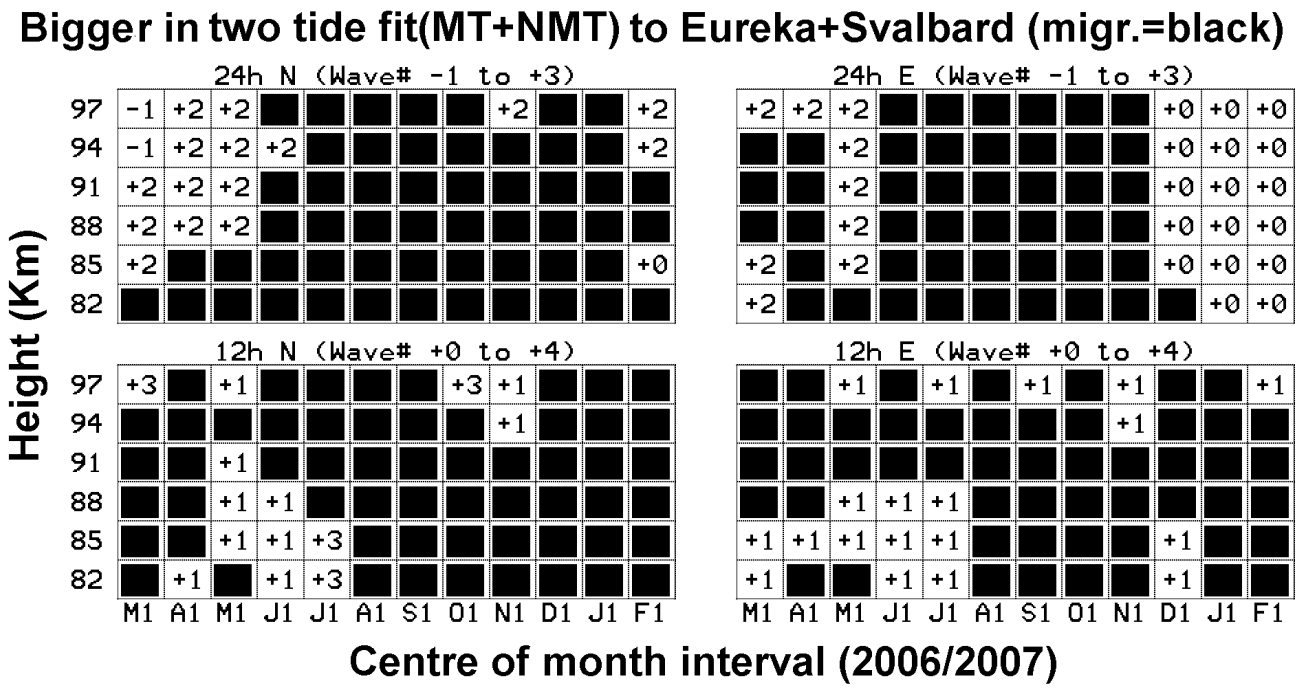

Fig. 9. Two-tide fits, using the wave numbers of the MT plus one of a range of NMT, were used to find the bigger: either the MT, which is shown here in black, or the NMT wave number in the ranges shown. The latter are appropriate to non-linear interaction with the SPW S=1 or 2.

height-month location is black. Wave numbers s=−1 to +3 were selected for the D tide, which is the range encompassed by MT s=1 plus and minus Stationary Planetary Wave (SPW) wave numbers S=1, 2. Correspondingly, for the SD tide wave numbers s=0 to +4 were selected, which is the range for MT s=2 plus and minus SPW S=1, 2. The rationale for using these SPW as participants in non-linear wave interactions is discussed in more detail below and in Sect. 6; one simple and statistical reason is to limit possible spurious wave number results. Finally we note that the dominant tides (MT or NMT) shown for the monthly fits in Fig. 9 were strongly confirmed by careful assessment of the results from fits to 4-day intervals. These latter showed significant clusters of particular "dominant tides", in both height and time, which favoured the relative simplicity of the version with monthly fits (Fig. 9). Minimal extra information has been eliminated by this choice.

The dominance of the zonal D tide's standing wave s=0 during the winter of 2006/07, and the SD tide's wave number s=+1 are clearly evident in Fig. 9. This relative importance of the NMT and MT is consistent with Fig. 8 and associated earlier discussion. For example the zonal diurnal phase-differences of 6–8 h of LT (pink color) for the observed tides from the Arctic radars in December–February correspond to zero hours UT, which is appropriate to NMT wave number zero (s=0, a tidal vacillation). Figure 9 shows a dominant zero wave number in that area. Small amplitude ratios S/E for the observed zonal tides from the Arctic radars (Fig. 8) have already been noted at those times and heights. The occurrence of this NMT in the zonal but not the meridional component is interesting: analysis of data from GCMs with data assimilation, and of Hough modes present in the observed s=0 NMT (e.g. Forbes and Wu, 2006) may shed light upon this matter. Also, the SD phase-differences of circa 2.5 h of LT for 82–90 km in May–June (Fig. 8), converted to UT difference, provide a phase-speed consistent with a wave number s=1, which is also featured dominantly and locally in Fig. 9. Small amplitude ratios S/E have already been noted at those times and heights in the comparison of the tides from the Arctic radars in Fig. 8. Again from that figure, there are additional height-time locations of SD s=+1, plus a few s=+3 in Fig. 9, which are consistent with larger Svalbard amplitudes at mainly 94–97 km.

The large regions of heights and months with small phase-differences in Fig. 8, which were discussed earlier and suggested as being prime candidates for MT-dominance, are generally also the black MT regions (s=1, diurnal; s=2, semidiurnal) in Fig. 9.

Non-linear interactions between SPW and migrating solar tides have often been discussed in the literature (e.g. Manson et al., 2004a; Aso, 2007), but nowhere better than by Hagan and Roble (2001). Hence and congruent with the software-logic used for the production of Fig. 9, interactions between the 12-h migrating tide and the SPW S=1 would provide

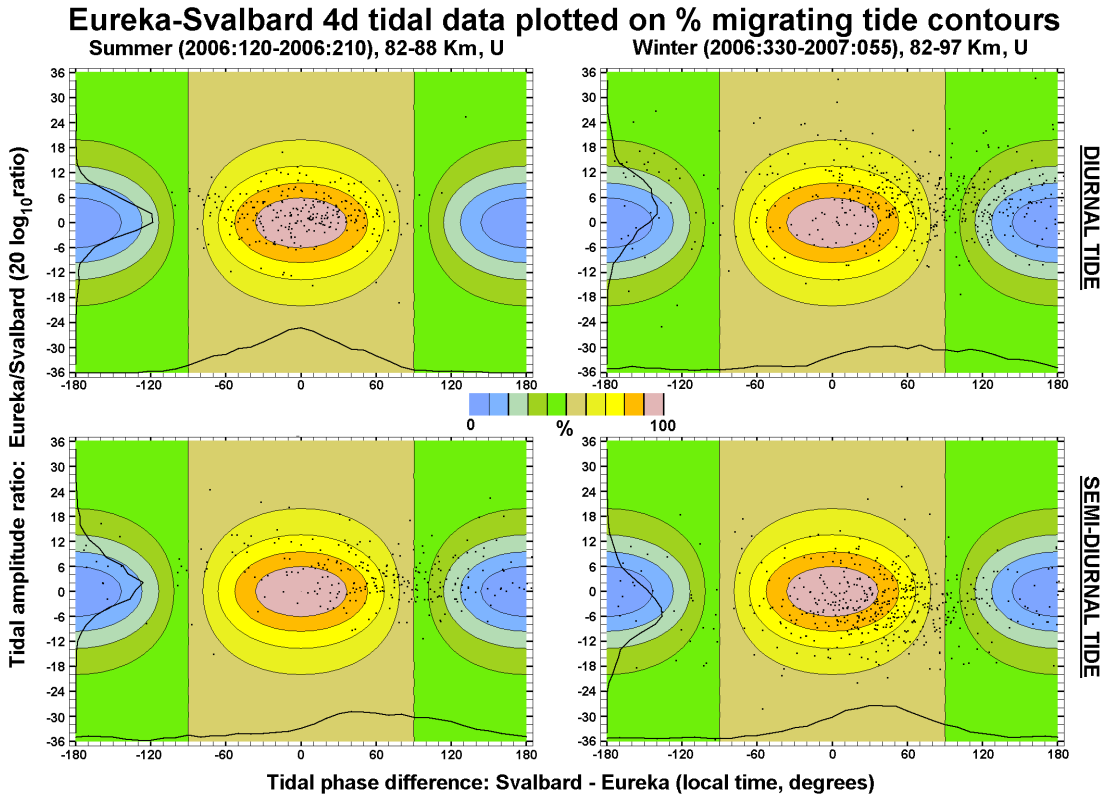

Fig. 10. Tidal amplitude ratios for the observed tides at Eureka and Svalbard versus their observed phase differences for the diurnal and semidiurnal tides. Model values are contoured in color (the scale is included in the figure), and 4-day observed tidal amplitude ratios are added as black dots.

NMT s=+1, +3; and the 24-h MT interactions with SPW S=1 would provide NMT s=0, +2. Consistent with this, there is an important additional feature in Fig. 9, and that is the dominance of NMT s=+2 for the diurnal tide of March-May, especially for the meridional component. The SPW S=1 is therefore favoured statistically as a prerequisite for the NMT displayed in Fig. 9.

Finally in this section we provide another visualization, which also illustrates the scatter of individual (4 day) amplitude ratios and phase differences for the two radar-locations (Fig. 10). Given any chosen amplitude ratio of the tides at the two radars (E/S) between +/−36 deciBels (dB), and any phase difference (S-E) between $\pm 180^o$, the percentage power in the migrating tide can be obtained analytically. Explicitly, the percentage power is the square of the MT amplitude compared with the mean summed squares of the tidal amplitudes at Eureka and Svalbard. There are four sections in Fig. 10: the east-west wind component of the 24-h and 12-h tides for a summer and winter interval. The percentage power for the MT is contoured in colours.

As expected the percentage is 100% for the amplitude ratio E/S=1 (0 dB) and phase-differences of zero degrees. As the phase-difference changes between zero and at ±180° the % power is reduced, becoming zero at ±180°. For zero phase-differences, the percentage becomes smaller as the amplitude ratio departs from unity (larger or smaller).

The observed amplitude ratios and phase differences for the Eureka and Svalbard tides, due to individual fits to 4-D sequences and 3–6 heights, have been super-imposed upon these model contours; the examples chosen for Fig. 10 involve data for May–July and December–February. Zonal components of the winds are shown. Choices of heights and months can be usefully compared with the table (Fig. 9) of "Biggest in two tide fit (MT+NMT)". In May–July, the 24-h tide values are centered upon zero phase difference, and amplitudes ratios close to unity (Eureka is larger by 1–2 dB as also evident in Fig. 8). The MT tide is clearly dominant, and consistent with this, the height-month locations of Fig. 9 are dominated by black (MT), with merely a hint of NMT (+2). The scattering of points will be due to noise in the tidal fits, variability due to the other and smaller NMT, and/or general atmospheric variability. The NS component plot, not shown, is almost identical. The 12-h tide data-points for this interval are spread between plus 20 and 120°, consistent with the influence of NMT; Fig. 9 has +1 as the dominant NMT in these height-month intervals. Eureka amplitudes are larger by 2 dB, as also shown in the tidal amplitude ratios of Fig. 8.

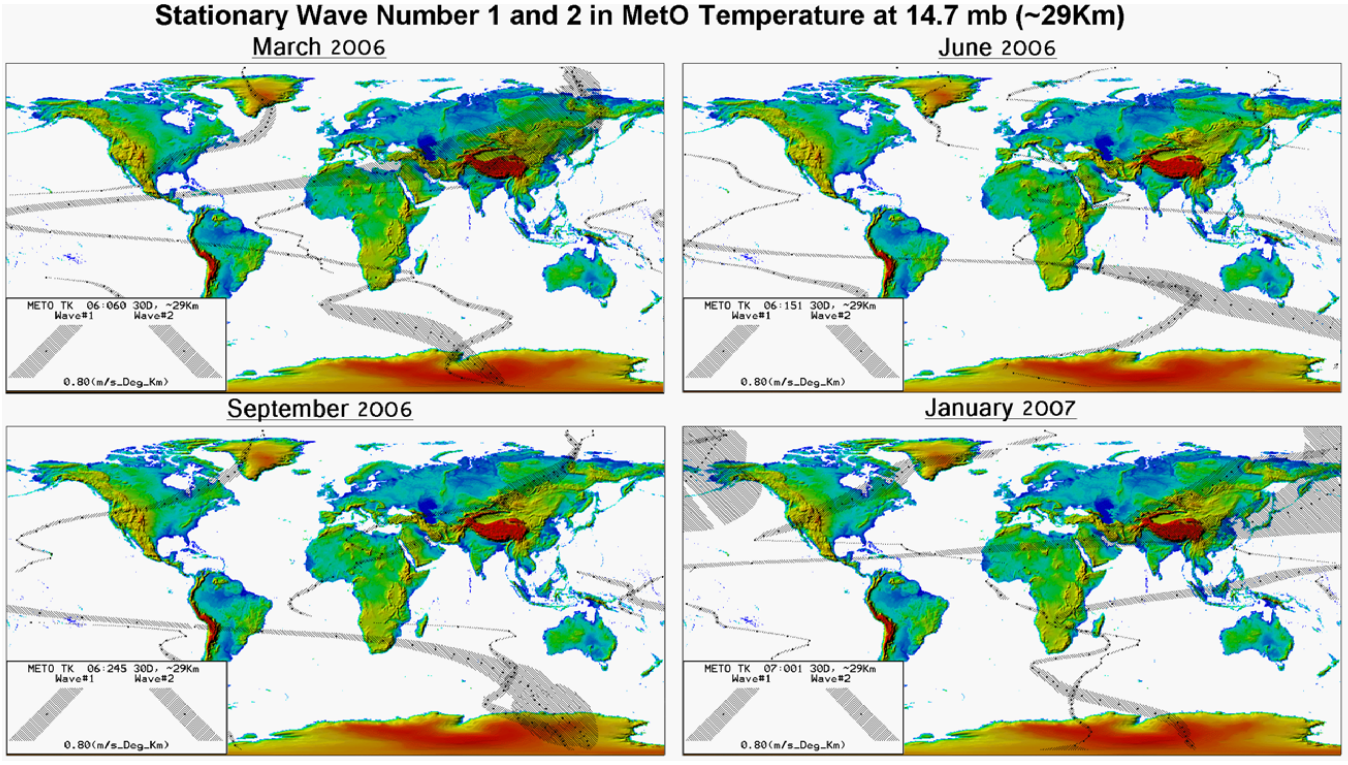

Fig. 11. Topographical global map: grey is sea level, and the Himalayas are 10 km (USGS). The 29 km atmospheric temperatures from MetO for the 4 seasons of the year provide pole to pole amplitudes of SPW S=1 and 2. The width of the hatched area perpendicular to the orientation of the line(s) of maximum temperature shows the amplitude of zonal stationary planetary waves S=1 and 2 in MetO-temperature. The hatch-widths given in the bottom left corner of each panel show the amplitude scale. Here the shown hatch-widths represent 0.8 degrees (K). The two slants of hatching are for S=1 (NW-SE) and 2 (SW-NE), and both positions of maxima are shown for S=2.

Moving to the winter December–February (2006) interval in Fig. 10, all six heights are combined. The data-points for the 24-h tide (EW) are distributed rather evenly about 90° phase difference, consistent with the dominance of NMT s=0, since the two radars are separated by ∼6 h (6.7) in Co-ordinated Universal Time (101° of longitude). This was expected because the height-month locations of Fig. 9 are dominated (17 of 18 possibilities) by the wave number s=0. Eureka amplitudes are larger than Svalbard by 2–4 dB (as in Fig. 8). The 12-h tide's data points lie mainly within the 70–100% contours suggesting MT dominance; in Fig. 9 black squares dominate (14 of 18) for the EW tide, with the remaining few s=+1. This dominance of MT is also the case for the NS tide (not shown in Fig. 10). The offset of phases from zero is due to the NMT influence. Svalbard 12-h tidal amplitudes are larger than those at Eureka, which is the outstanding feature for this first year of observations.

6 Forcing of the Stationary Planetary Waves (SPW)

As discussed within the tidal papers referenced in the Introduction, SPW are the prime polar latitude candidates for forcing of the NMT through non-linear interactions with the solar migrating tides. The modulation of the 12-h and 24-h harmonics of solar absorption, which includes such processes as deep convection and latent heating, by the dominant zonal wave numbers in the Earth's topography, result in the majority of the NMT (Forbes et al., 2003; Manson et al., 2004a). Although such topographical forcings are inherently included in atmospheric GCMs, they have seldom been analytically included in tidal papers. We used topographic data from US Geological Survey's website to produce a global plot of surface altitudes (90° S to 90° N, 0–360° E), Fig. 11. The analytical topographic wave numbers are as follows: weakest spectra are near the equator (±15°) and southern extra-tropical oceanic latitudes (35–65° n=1, 3); Oceania has minor n=1 and 4 peaks; the Northern Hemisphere's (NH) outstanding features are due to the dominant Himalayas (a broad n=1–2 peak and then weaker peaks at n=4 and beyond), which blends into that of Greenland (an n=1 peak, tapering smoothly to higher values of n). There is a significant phase shift between the topographical wave numbers due to these two mountainous structures, and this will also be expected in the atmospheric waves yet to be

discussed. Antarctica remains for comment, and it is much less symmetrical than many discussions of the southern polar vortex would suggest: there is a strong peak at n=1 and then a smaller peak at n=3). Topography affects the positions, amplitudes and wave numbers of atmospheric SPW, due to seasonal variations in the relative temperatures of land and sea, but also the related forcing of tides due to latent heat and water vapour distributions (Manson et al., 2004a, 2006) and also ozone. This figure and the discussion above are a beginning to a topic that will require significant research: relationships between the boundary layer, surface science and the atmosphere. Our assessment is that GCMs with data assimilation, with their inherent global and 3-D atmospheric structures, will be required to make significant progress. We are presently active in this area.

MetO (UK Meteorological Office) data from their data-assimilation GCM were then used for the months of 2006/07, to obtain the wave numbers of the atmospheric SPW. Plots (longitude versus latitude) for EW/NS wind and temperature at 10, 20, 30, 40, 55 km were inspected. Northern winter-like months (November to February) at circa 30 km provided a dominant S=1 in the extra-tropics, with longitudinal phase differences of $>180^\circ$ consistent with the topographical features of the Himalayas at middle latitudes and Greenland at high latitudes. Spectra also evidenced less, but significant, energy at S=2, 3 at middle latitudes, due to the richness of the topographic spectra (Himalayas plus Rocky Mountains). There was very weak spectral energy at high polar latitudes of the SH. The northern summer-like months (June–September) provided spectra that had maxima in the Southern Hemisphere's winter (significantly smaller than the NH winter), and with only very modest spectral presence in the NH. The equinoxes, most obviously March–May and October-November, evidenced spectral energy in both hemispheres mainly at S=1. The weaker global winds but with westerlies in both hemispheres (Chshyolkova et al., 2006), have allowed the SPW to propagate globally. As noted in that paper, propagation of transient 16-d waves (m=1) also then occurs.

This material is summarized in Fig. 11: the amplitudes of the MetO-derived SPW S=1 and 2 (distinguished by "NW-SE" and "SW-NE" hatching of the band respectively at 29 km) and phase location (longitude) of the wave maxima are provided for two solstitial and equinoctial months. January has the largest NH S=1 amplitudes, while June has SH S=1 maxima, significantly smaller than these of January. March and September, which are the nearest equinoctial months to the respective hemispheric winters, have significant S=1 amplitudes globally, but are largest in the NH and SH respectively (Chshyolkova et al., 2006), The dominant wave numbers of the atmospheric SPW are consistent with the dominant topographical wave numbers, with wave number one generally being the largest in Fig. 11. We conclude this section with direct comparisons between the SPW amplitudes and the MT and NMT data discussed earlier.

The SPW wave number S=1 amplitudes for high latitudes of both hemispheres, from 4 day fits that are shifted by 1 day, are shown in Fig. 12. The meridional wind component is used, but zonal winds or temperatures perturbations are similar in seasonal and monthly variations. It is immediately obvious that during the winter months of each hemisphere the Arctic amplitudes are much larger than those in the Antarctic. Consistent with these amplitudes, as they relate to wave propagation, the zonal winds are eastward from 40–97 km in the Northern Hemisphere during the months September to April, while they are eastward in the Southern Hemisphere during the months March–October. During the early spring months of September–October for the south the SPW amplitudes are largest. This is associated with the dominant and final stratospheric warmings of the Southern Hemisphere, which may be comparable in dynamical intensity and complexity to the mid-winter warmings of the Northern Hemisphere. In Fig. 12 the stratospheric warming events occurred during January and February.

Time sequences of the percentage-power of the migrating tide for both the 24-h and 12-h tides, as obtained from the Eureka and Svalbard radars, are also shown in Fig. 12. The NS component has been chosen. For the 24-h tide, this figure illustrates the dominance of the MT in the summer and early autumn months (June–October), with values very close to 100%. This higher time-resolution figure and statement are consistent with the monthly means of Fig. 9. Sequences for the 24-h EW component are not shown, but are similar to these for the NS. Considering the 12-h tides, the sequences in Fig. 12 show MT dominance for the three upper heights in June–July, and then almost exclusively for all heights from August through to the middle of winter (January). The exceptions are NMT presence for the upper heights in October–November; the monthly values in Fig. 9 are similar to this. During this equinoctial time the SPW amplitudes in both hemispheres are comparable, so global forcing of the NMT is possible. Behavior of the 12-h EW component, which is not shown, is similar to the NS component, as suggested by the monthly states in Fig. 9.

It is important to note that there is not a clear peak to peak correspondence between the SPW amplitudes shown, and the % powers of the MT. Interactions between the SPW and the MT tides will occur on a global or at least hemispheric scale (Hagan and Roble, 2001), and the temporal and spatial aspects of these interactions are best dealt with using specific models (Aso, 2007; and note the discussions in the Introduction, Sect. 1), and realistic GCMs and specific experiments with year-specific data assimilation. There is very little indication from Fig. 12 that the Antarctic-winter SPW, which are relatively small, are responsible for significant NMT activity in the Arctic summer. Indeed, given the strong NMT activity in the Arctic-winter and spring that we are now reporting, when the local SPW are large, it is very likely that the prominent and observed NMT activity of the Antarctic-summer (Murphy et al., 2006; Baumgaertner et al., 2006; 12-h NMT

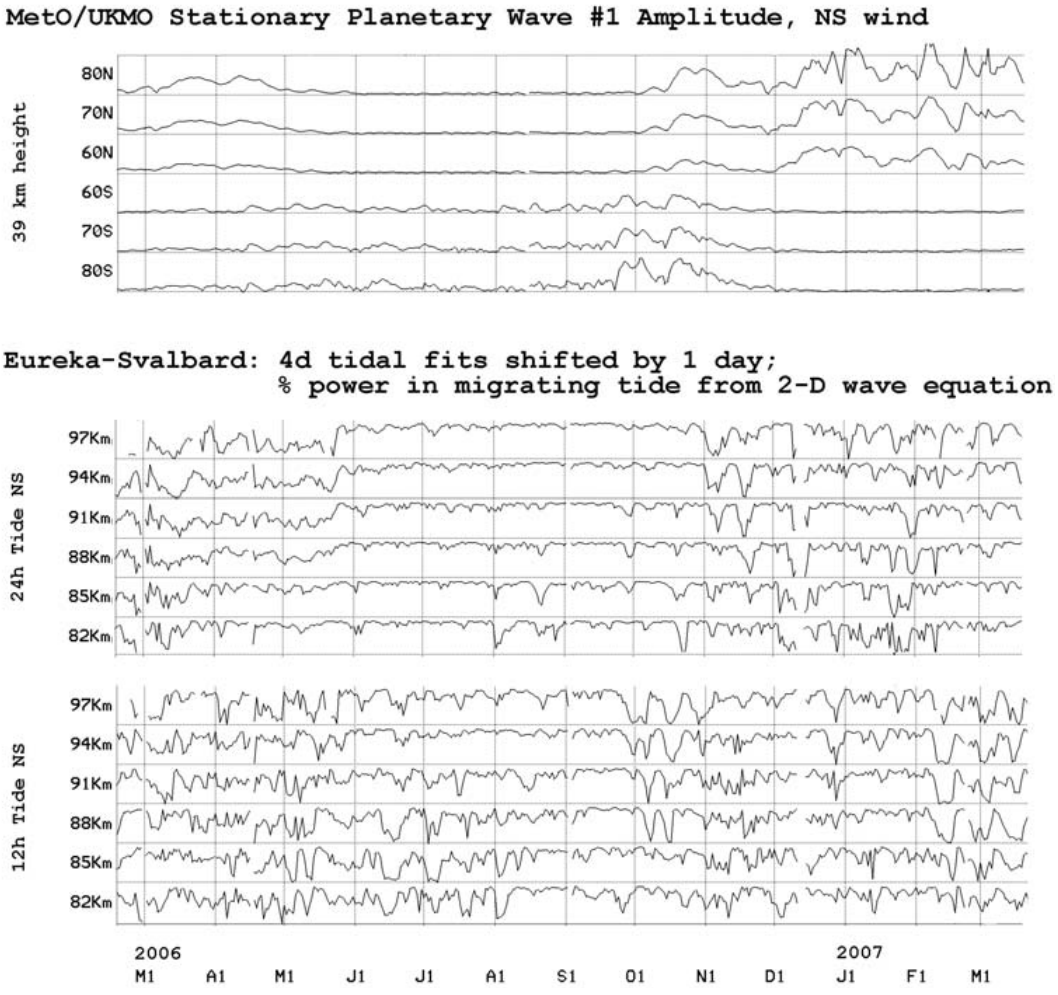

Fig. 12. Time-sequences of the amplitude, obtained from the Fourier transform, for the SPW S=1 (80 m/s for each height-box/sequence): in this case the NS component of the wind, at high latitudes of both hemispheres and at 39 km, is shown. Below, and using the same analysis as used for Figs. 9 and 10, we show the % power in the MT when compared with the RMS of the observed tides at Eureka and Svalbard.

s=+1 as discussed in Sect. 1) is associated with the global presence of these NMT. The reverse (SPW from the SH winter driving the 12-h NMT s=+1 at 78–80° N) appears not to be the case, despite the claims of Smith et al. (2007): the latter is the subject of scrutiny in an extended study by the present authors, with significance-levels being a source of serious concern.

7 Planetary waves

We provided a brief introduction to planetary waves in the 2–20 day range with Figs. 1 and 3 of Sect. 3. A larger, likely three year, data set is needed to gather enough oscillations of these transient features to provide useful generalizations.

However readers will expect a further figure and comment on non-stationary Planetary Waves (PW). We provide wavelets in Fig. 13 for the annual variations of the EW and NS winds at 88 km over the 12 months of 2006: a detailed description of the analysis method for the wavelet is provided in Manson et al. (2005). These are for Eureka, Svalbard and southern neighbor Tromso, as well as for Saskatoon whose PW data have often been compared to Tromso (we collaboratively operate the Tromso and Eureka radars). At the 78/80° N sites there is spectral energy up to long periods of 10–20 days during the winter-like months (October to March) and 2–5 days for the summer-centred months. A likely shared feature at the four radars is a 5-day oscillation in the zonal wind near day 300 (it is smallest at Tromso). Perfect agreement between PW spectral features at several radars is surprisingly rare (Luo et al., 2002). The spectral occurrences of the large features (green, yellow-green) at Tromso are generally quite similar to Svalbard, and certainly not stronger. The 5–10 day feature in January is common. The ubiquitous summer-centred 2-d wave is strongest at Saskatoon, where the “dish” shaped yellow-red colors

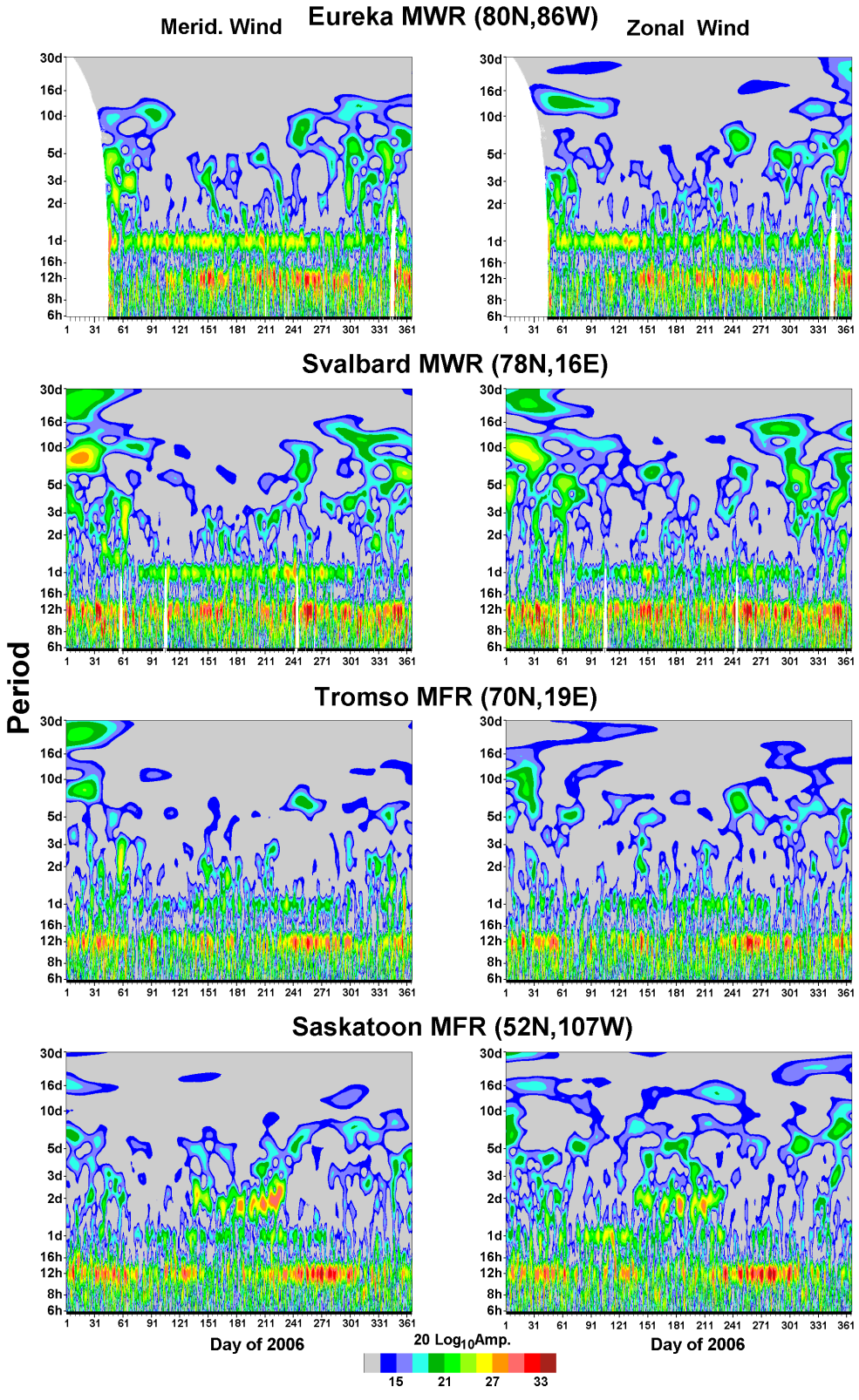

Fig. 13. Wavelet analyses applied to winds data from the two Arctic radars, Tromso and Saskatoon. The analysis method is described fully in Manson et al. (2005). The dominance of the semidiurnal tide at Svalbard and the diurnal tide at Eureka is clearly evident. Planetary wave activity is relatively strong in the Arctic.

(smallest period in mid- summer) is clearest in the meridional (NS) component. At Tromso the feature is weaker (green with speckles of yellow), but still dish shaped in the NS component. It becomes progressively weaker at the 78–80° N locations. The differences between spectral features at Svalbard and Eureka, in time of occurrence and frequency, are typical of those already observed at middle latitudes (Manson et al., 2005; Chshyolkova et al., 2005).

The number of oscillations occurring during a typical burst of Rossby wave activity (Luo et al., 2002) is small, so that these PW are best studied over several years and then for a range of latitudes. Such is our intention.

8 Summary with discussion

The discussions throughout this paper have been quite detailed, so we will not extend them here. A few observations in summary are desirable however. We have provided the first comparison of height (82–97 km) versus time (12 months of 2006/07) contour plots of diurnal (D) and semidiurnal (SD) tidal amplitudes and phases at two, effectively equal, latitudes (78° N, 80° N) and usefully differing longitudes (16° E and 86° W).

1. The first two (AHM, CEM) authors noted from the very beginning of Canadian observations at Eureka (80° N) that the tidal amplitudes were larger than expected, and that the relative magnitudes of the 24-h and 12-h tides differed from these at Saskatoon, Canada (52° N). Existing expectations were based upon Saskatoon and Tromso (70° N) observations (Manson et al., 2002, 2004c). Unique polar information on diurnal non-migrating tides (NMT) has been provided, as well as complementary information to that existing for the Antarctic on the semidiurnal NMT. While just two locations/radars have been used, the consistency with time and height of the wave numbers provided for the diurnal and semidiurnal NMT, and their excellent matching with wave numbers appropriate to forcing by non-linear interactions between the MT and SPW, are excellent evidence for the reality of these NMT. Data from three or more locations would provide relative magnitudes of the NMT, without any limitations regarding the forcing mechanism for the NMT.

2. Longitudinal variability of the Arctic tides (78/80° N) became more apparent as Svalbard tides were assessed for the year March 2006–February 2007. The radars are of effectively identical characteristics. In general terms the 12-h tide as observed (combinations of MT and NMT) at Svalbard was larger than at Eureka, although phases (contour-colors) if not their gradients were often similar (within 1–2 h), except during the equinoxes. In contrast the observed 24-h tide at Eureka was generally larger, and the phases at the two sites differed in both vertical and time (monthly) gradients, especially in the winter and spring months. The seasonal variations of the diurnal and semidiurnal tides, in height and time, differed between Eureka and Svalbard.

3. Hodograph analysis showed that for the diurnal tide the strong amplitudes-differences between the Arctic latitudes of Norway and Canada were partly associated with the dominance at Svalbard of elliptical oscillations of large axial ratio and preferred north-south orientations.

4. Fitting of migrating and non-migrating tides (MT, NMT) to the data illustrated very convincingly that the NMT were often larger than the MT: during spring (March–May) and then winter (December–February) for the 24-h tide (s=+2 and 0); and then spring and early summer (March–July) at low heights, and more weakly in the autumn (September–November) for the 12-h tide (s=+1 and occasionally +3). The NMT wave numbers are fully consistent with stationary planetary wave SPW S=1 non-linear interactions with the MT tides. The presence of these NMT is usefully consistent with the paper by Forbes and Wu (2006), discussed in the Introduction, which provided UARS-MLS temperature tides (1991–1997) up to 70° N. However the Arctic spring and winter tidal winds shown here for 2006/07 at ∼80° N have larger diurnal s=0,+2 NMT relative to the MT, in contrast with the MLS tides at 70° N and 86 km; and the semidiurnal s=1 NMT Arctic monthly occurrences do not coincide well with the MLS tides at 70° N. Interannual variations of the MT and NMT at Svalbard and Eureka will be investigated after the completion of the second IPY year, March 2009. There are certainly physical expectations based upon variable forcing mechanisms e.g. the SPW, and already good evidence that interannual variations may be significant (Hagan and Forbes, 2003; Baumgaertner et al., 2006; Wu et al., 2008)

5. Spatial Fourier spectra of the planet's topography and also of the atmosphere (from the GCM with data assimilation, MetO), demonstrate the dominance of wave numbers 1 and the smaller 2. Greenland dominates the topographic forcing of the Arctic SPW S=1. The SPW of the stratosphere near 30 km are larger in the Arctic winter than in the Antarctic winter, and during the equinoxes these waves exist globally.

6. The Arctic tides demonstrate dominantly MT behaviors for the diurnal tide in summer and early fall when the local SPW amplitudes are small. There is thus little to no indication of significant NMT forcing from the Southern Hemisphere's winter SPW, which by the SH spring have reached their annual maximum. Global presence of SPW in September–October and more modestly in

April–May may lead to the presence of the Arctic NMT (s=+1 and +3) for the 12-h tide, whose seasonal variability is closer to being equinoctial. It is probable that the large SPW of the NH winter and their associated NMT are linked through trans-equatorial propagation to the reported/observed summer semidiurnal NMT of Antarctica. Radar data from the SH will be sought for the next study of Arctic tides, which will involve interannual variability, GCM models with data assimilation, as well as global distributions of forcing chemical species (ozone and water vapour).

7. The transient planetary waves have comparable amplitudes to those at lower high-middle latitudes. They also demonstrate some longitudinal variations between Norway and Canada, and the presence of the longest periods (10–20 days) in winter-like months. Several years of data are required to investigate these transient features.

Acknowledgements. We are grateful to the British Atmospheric Data Centre (BADC) for access to MetO data. The Canadian Network for the Detection of Atmospheric Change (CANDAC), along with its Principal Investigator Professor James Drummond, are thanked profoundly for the provision of salary support (CEM, TC) and for the operation and maintenance of the radar at Eureka (Polar Environment Atmospheric Research Laboratory, PEARL). The Canadian authors acknowledge research support through grants from the Natural Sciences and Engineering Council (NSERC), research funding from the Canadian Foundation for Climate and Atmospheric Science (CFCAS), and support from their individual Universities, Departments and Institutes.

Editor in Chief W. Kofman thanks M. J. Jarvis and two other anonymous referees for their help in evaluating this paper.

References

Aso, T.: Penetration of the non-migration atmospheric diurnal tide into polar latitudes, Adv. Polar Upper Atmos. Res., 14, 138–145, 2000.

Aso, T.: A note on the semidiurnal non-migrating tide at polar latitudes, Earth Planets Space, 59, 21–24, 2007.

Baumgaertner, A. J. G., McDonald, A. J., Fraser G. J., et al.: Long-term observations of mean winds and tides in the upper mesosphere and lower thermosphere above Scott Base, Antarctica, J. Atmos. Solar-Terr. Phys., 67(16), 1480–1496, 2005.

Baumgaertner, A. J. G., Jarvis, M. J., McDonald, A. J., et al.: Observations of the wave number 1 and 2 components of the semidiurnal tide over Antarctica, J. Atmos. Solar-Terr. Phys., 68(11), 1195–1214, 2006.

Chshyolkova, T., Manson, A. H., Meek, C. E., Avery, S. K., Thorsen, D., MacDougall, J. W., Hocking, W., Murayama, Y., and Igarashi, K.: Planetary wave coupling in the middle atmosphere (20–90 km): A CUJO study involving TOMS, MetO and MF radar data, Ann. Geophys., 23, 1103–1121, 2005, http://www.ann-geophys.net/23/1103/2005/.

Chshyolkova, T., Manson, A. H., Meek, C. E., Avery, S. K., Thorsen, D., MacDougall, J. W., Hocking, W., Murayama, Y., and Igarashi, K.: Planetary wave coupling processes in the middle atmosphere (30–90 km): a study involving MetO and MF radar data, J. Atmos. Solar-Terr. Phys., 68, 353–368, 2006.

Chshyolkova, T., Manson, A. H., Meek, C. E., Aso, T., Avery, S. K., Hall, C. M., Hocking, W., Igarashi, K., Jacobi, C., Makarov, N., Mitchell, N., Murayama, Y., Singer, W., Thorsen, D., and Tsutsumi, M.: Polar vortex evolution during Northern Hemispheric winter 2004/05, Ann. Geophys., 25, 1279–1298, 2007, http://www.ann-geophys.net/25/1279/2007/.

Cierpik, K. M., Forbes, J. M., Miyahara, S., Miyoshi, Y., Fahrutdinova, A., Jacobi, C., Manson, A. H., Meek, C., Mitchell, N. J., and Portnyagin, Y.: Longitude variability of the solar semidiurnal tide in the lower thermosphere through assimilation of ground- and space-based wind measurements, J. Geophys. Res., 108(A5), 1202, doi:10.1029/2002JA009349, 2003.

Forbes, J. M., Makarov, N. A., and Portnyagin, Y.: First Results from the Meteor Radar at South-pole – A large 12-hour Oscillation with Zonal wave-number one, Geophys. Res. Lett., 22(23), 3247–3250, 1995.

Forbes, J. M., Zhang, X. L., Talaat, E. R., and Ward, W.: Nonmigrating diurnal tides in the thermosphere, J. Geophys. Res.-Space Phys., 108(A1), 1033, doi:10.1029/2002JA009262, 2003.

Forbes, J. M. and Wu, D.: Solar tides as revealed by measurements of mesosphere temperature by the MLS experiment on UARS, J. Atmos. Sci., 63(7), 1776–1797, 2006.

Hagan, M. E. and Roble, R. G.: Modeling diurnal tidal variability with the National Center for Atmospheric Research thermosphere-ionosphere-mesosphere-electrodynamics general circulation model, J. Geophys. Res.-Space Phys., 106(A11), 24869–24882, 2001.

Hagan, M. E. and Forbes, J. M.: Migrating and nonmigrating semidiurnal tides in the upper atmosphere excited by tropospheric latent heat release, J. Geophys. Res.-Space Phys., 108(A2), 1062, doi:10.1029/2001JD001236, 2003.

Hall, C. M., Aso, T., Manson, A. H., et al.: High-latitude mesospheric mean winds: A comparison between Tromso (69 degrees N) and Svalbard (78 degrees N), J. Geophys. Res.-Atmos., 108(D19), 4598, doi:10.1029/2003JD003509, 2003.

Hall, C. M., Aso, T., Tsutsumi, M., Nozawa, S., Manson, A. H., and Meek, C. E.: A comparison of mesosphere and lower thermosphere neutral winds as determined by meteor and medium-frequency radar at 70° N, Radio Sci., 40, RS4001, doi:10.1029/2004RS003102, 2005.

Hernandez, G., Fraser, G. J., and Smith, R. W.: Mesospheric 12-hour Oscillation near South-pole, Antarctica, Geophys. Res. Lett., 20(17), 1787–1790, 1993.

Hocking, W. K.: A new approach to momentum flux determinations using SKiYMET meteor radars, Ann. Geophys., 23, 2433–2439, 2005, http://www.ann-geophys.net/23/2433/2005/.

Luo, Y., Manson, A. H., Meek, C. E., Thayaparan, T., MacDougall, J. W., and Hocking, W.: The 16-day wave in the mesosphere and lower thermosphere: simultaneous observations at Saskatoon (52° N, 107° W) and London (43° N, 81° W), Canada, J. Atmos. Solar-Terr. Phys., 64, 1287–1307, 2002.

Manson, A. H., Meek, C. E., Koshyk, J., Franke, S., Fritts, D. C., Riggin, D., Hall, C. M., Hocking, W. K., MacDougall, J., Igarashi, K., and Vincent, R. A.: Gravity wave activity and dynamical effects in the middle atmosphere (60–90 km): observations from an MF/MLT radar network, and results from the Cana-

dian Middle Atmosphere Model (CMAM), J. Atmos. Solar-Terr. Phys., 64, 65–90, 2002.

Manson, A. H., Meek, C., Hagan, M., Zhang, X., and Luo, Y.: Global distributions of diurnal and semidiurnal tides: observations from HRDI-UARS of the MLT region and comparisons with GSWM-02 (migrating, nonmigrating components), Ann. Geophys., 22, 1529–1548, 2004a, http://www.ann-geophys.net/22/1529/2004/.

Manson, A. H., Meek, C. E., Hall, C. M., Nozawa, S., Mitchell, N. J., Pancheva, D., Singer, W., and Hoffmann, P.: Mesopause dynamics from the scandinavian triangle ofradars within the PSMOS-DATAR Project, Ann. Geophys., 22, 367–386, 2004b, http://www.ann-geophys.net/22/367/2004/.

Manson, A. H., Meek, C. E., Chshyolkova, T., Avery, S. K., Thorsen, D., MacDougall, J. W., Hocking, W., Murayama, Y., Igarashi, K., Namboothiri, S. P., and Kishore, P.: Longitudinal and latitudinal variations in dynamic characteristics of the MLT (70–95 km): a study involving the CUJO network, Ann. Geophys., 22, 347–365, 2004c, http://www.ann-geophys.net/22/347/2004/.

Manson, A. H., Meek, C. E., Chshyolkova, T., et al.: Wave activity (planetary, tidal) throughout the middle atmosphere (20–100 km) over the CUJO network: Satellite (TOMS) and Medium Frequency (MF) radar observations, Ann. Geophys., 23, 305–323, 2005, http://www.ann-geophys.net/23/305/2005/.

Manson, A. H., Meek, C., Chshyolkova, T., McLandress, C., Avery, S. K., Fritts, D. C., Hall, C. M., Hocking, W. K., Igarashi, K., MacDougall, J. W., Murayama, Y., Riggin, C., Thorsen, D., and Vincent, R. A.: Winter warmings, tides and planetary waves: comparisions between CMAM (with interactive chemistry) and MFR-MetO observations and data, Ann. Geophys., 24, 2493–2518, 2006, http://www.ann-geophys.net/24/2493/2006/.

Murphy, D. J., Forbes, J. M., Walterscheid, R. L., Hagan, M. E., Avery, S. K., Aso, T., Fraser, G. J., Fritts, D. C., Jarvis, M. J., McDonald, A. J., Riggin, D. M., Tsutsumi, M., and Vincent, R. A.: A climatology of tides in the Antarctic mesosphere and lower thermosphere, J. Geophys. Res.-Atmos., 111(D23), D23104, doi:10.1029/2005JD006803, 2006.

Nozawa, S., Brekke, A., Manson, A., Hall, C. M., Meek, C., Morise, K., Oyama, S., Dobashi, K., and Fujii, R.: A comparison study of the auroral lower thermospheric neutral winds derived by the EISCAT UHF radar and the Tromso medium frequency radar, J. Geophys. Res., 107(A8), 1216, doi:10.1029/2000JA007581, 2002.

Oberheide, J. and Forbes, J. M.: Tidal propagation of deep tropical cloud signatures into the thermosphere from TIMED observations, Geophys. Res. Lett., 35(4), L04816, doi:10.1029/2007GL032397, 2008.

Portnyagin, Y. I., Forbes, J. M., Makarov, N. A., Merzlyakov, E. G., and Palo, S.: The summertime 12-h wind oscillation with zonal wavenumber $s = 1$ in the lower thermosphere over the South Pole, Ann. Geophys., 16, 828–837, 1998, http://www.ann-geophys.net/16/828/1998/.

Portnyagin, Y. I., Solovjova, T. V., Makarov, N. A., et al.: Monthly mean climatology of the prevailing winds and tides in the Arctic mesosphere/lower thermosphere, Ann. Geophys., 22, 3395–3410, 2004, http://www.ann-geophys.net/22/3395/2004/.

Riggin, D. M., Meyer, C. K., Fritts, D. C., Jarvis, M. J., Murayama, Y., Singer, W., Vincent, R. A., and Murphy, D. J.: MF radar observations of seasonal variability of semidiurnal motions in the mesosphere at high northern and southern latitudes, J. Atmos. Solar-Terr. Phys., 65(4), 483–493, 2003.

Smith, A. K., Pancheva, D. V., Mitchell, N. J., Marsh, D. R., Russell III, J. M., and Mlynczak, M. G.: A link between variability of the semidiurnal tide and planetary waves in the opposite hemisphere, Geophys. Res. Lett., 34, L07809, doi:10.1029/2006GL028929, 2007.

Wu, Q., Killeen, T. L., Nozawa, S., et al.: Observations of mesospheric neutral wind 12-hour wave in the Northern Polar Cap, J. Atmos. Solar-Terr. Phys., 65(8), 971–978, 2003.

Wu, Q., Ortland, D. A., Killeen, T. L., Roble, R. G., Hagan, M. E., Liu, H. L., Solomon, S. C., Xu, J. Y., Skinner, W. R., and Niciejewski, R. J.: Global distribution and interannual variations of mesospheric and lower thermospheric neutral wind diurnal tide: 2. Nonmigrating tide, J. Geophys. Res.-Space Phys., 113(A5), A05309, doi:10.1029/2007JA012543, 2008.

Yamashita, K., Miyahara, S., Miyoshi, Y., Kawano, K., and Ninomiya, J.: Seasonal variation of non-migrating semidiurnal tide in the polar MLT region in a general circulation model, J. Atmos. Solar-Terr. Phys., 64, 1083–1094, 2002.

Zhang, X. L., Forbes, J. M., Hagan, M. E., Russell III, J. M., Palo, S. E., Mertens, C. J., and Mlynczak, M. G.: Monthly tidal temperatures 20–120 km from TIMED/SABER, J. Geophys. Res.-Space Phys., 111(A10), A10S08, doi:10.1029/2005JA011504, 2006.